Australian Government
Bureau of Meteorology

Murray Basin — National Hydrological Projections Assessment report

Sri Srikanthan, Ulrike Bende-Michl, Vjekoslav Matic, Pandora Hope, Alison Oke, Zaved Khan, Steven Thomas, Wendy Sharples, Greg Kociuba, Justin Peter, Elisabeth Vogel, Louise Wilson, Margot Turner

ISBN 978-1-925738-42-1 Version 1.1 July 2022

Published by the Bureau of Meteorology

Cover image: Murray River at sunset – aerial view, Greg Brave, 18 November 2019

Contents

List of figures

List of tables

1 Introduction to the National Hydrological Projections

Australia's climate is changing: temperatures are increasing and precipitation patterns are shifting, as described in the *State of the climate 2020* (CSIRO & Bureau of Meteorology 2020). On average, Australia has warmed by 1.44 ± 0.24 °C since national records began in 1910. Streamflow has changed across the country, broadly increasing in the north and decreasing in the south. The *State of the climate 2020* reports that, in Australia's south-west, cool-season (May–October) precipitation has declined by around 16% since 1970. The decrease is even more pronounced for the winter months (May–July) for the same period. In the south-east of Australia, precipitation started to decline around 1990, and the average cool-season precipitation from 2000 to 2019 is now 12% less than last century (CSIRO & Bureau of Meteorology 2020). Along with this observed decline in precipitation, streamflow has declined substantially in both the south-west and south-east; changes in streamflow are typically disproportionally larger than changes in precipitation (Chiew 2006; Wasko et al. 2021; Zhang et al. 2016). In contrast, precipitation has increased across many northern parts of the country, and streamflow follows this trend (Zhang et al. 2016).

With rising greenhouse gas (GHG) levels in the atmosphere, temperature changes are projected to continue and intensify in the future, causing further warming and changes in all components of the climate and hydrological system (CSIRO & Bureau of Meteorology 2015). Given the limited water available for many Australian communities, businesses, governments and environments, these changes represent ongoing challenges to the management of Australia's water resources. The future security of our food and energy supplies, and our ecosystems, depends on water availability, as the demand for water is also growing.

To ensure that future water needs are met, decision-makers need forward-looking datasets and methods to evaluate a range of conceivable futures while accounting for uncertainty. The National Hydrological Projections product suite supports the process of strategic decision-making processes for future water resource management, adaptation and water policy developments. It consists of nationally consistent hydrological projections datasets, information and guidance material on future changes in Australia's projected hydrological variables.

The National Hydrological (NHP) Projections service complements projections work that has been undertaken by many federal and state governments, universities, and other organisations across Australia. A broad overview of available projections for Australia is given in Table 1.1. It is important to understand the varying nature of these projections including NHP in selected global climate models and their generation, greenhouse gas emission pathways, downscaling methods, spatial resolution, output variables and anticipated purpose ahead of their use. Further details about the Australian projections landscape, guidance material and readily available projections datasets can be found here: https://www.climatechangeinaustralia.gov.au/en/overview/about-site/landscape/

Table 1.1. Projections landscape for Australia

Name	State	Link
Climate Change in Australia	National	https://www.climatechangeinaustralia.gov.au/en/
Electricity Sector Climate Information	National	https://www.energy.gov.au/government-priorities/energy-security/electricity-sector-climate-information-esci-project
NSW and Australian Regional Climate Modelling project	New South Wales/Australian Capital Territory	https://climatedata-beta.environment.nsw.gov.au/
Climate Change NT	Northern Territory	https://climatechange.nt.gov.au/
Long Paddock	Queensland	https://www.longpaddock.qld.gov.au/qld-future-climate/
SA Climate Ready	South Australia	https://environment.sa.gov.au
Climate Futures for Tasmania	Tasmania	https://climatefutures.org.au/projects/climate-futures-tasmania/
Victorian Climate Projections 2019 Victorian Water and Climate Initiative	Victoria	https://www.climatechangeinaustralia.gov.au/en/projects/victorian-climate-projections-19 https://www.water.vic.gov.au/climate-change/reserach/vicwaci
Western Australian climate projections	Western Australia	https://www.wa.gov.au/government/publications/western-australian-climate-projections-summary

1.1 Developing the National Hydrological Projections

Broadly, the National Hydrological Projections were produced by choosing representative emission pathways (RCPs) and using a number of global climate model (GCM) inputs to run with a hydrological landscape water balance model (Figure 1.1).

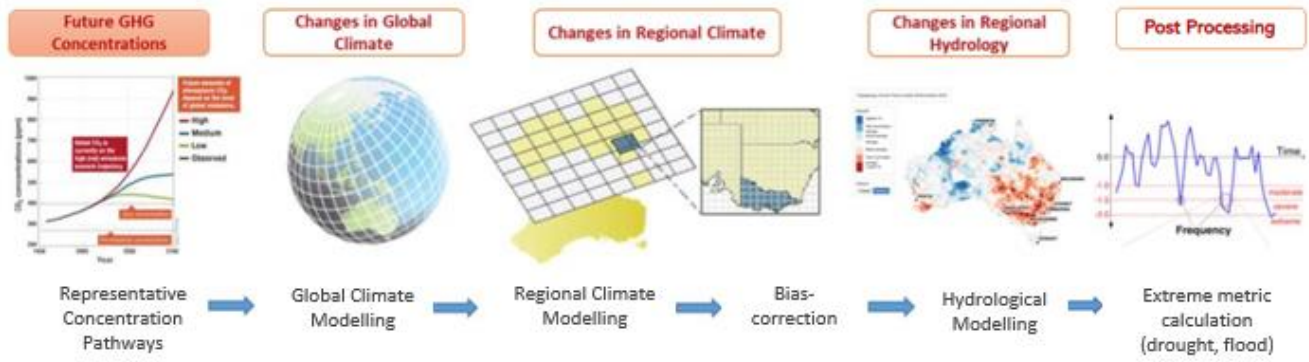

Figure 1.1. National Hydrological Projections workflow principles showing the processing steps: i) selecting representative concentration pathways, ii) running the 4 selected global climate models and also a regional climate model, iii) correcting the discrepancies between climate input and observation (bias correction) to produce the climate data, iv) running the climate data through a hydrological model to project hydrological changes and v) calculating projected hydrological extremes

State-of-the-art techniques were used to resolve the climate data to a finer geographic scale and correct for biases (to adjust for discrepancies between observations and the climate models). The resultant climate data was processed through a hydrological model to produce projections of future hydrological changes and extreme conditions.

Australian and international climate modelling groups simulate the world's weather and climate with global climate models under historical and future forcing from greenhouse gases as well as from atmospheric and solar forcing ('forcing' is the term used to describe the impacts of factors that affect Earth's climate). The models used for the National Hydrological Projections stem from the Coupled Model Intercomparison Project Phase 5 (CMIP5) (Taylor et al. 2012) undertaken by the World Climate Research Programme's Working Group on Coupled Modelling (WGCM) (PCMDI 2021).

First, 2 future scenarios were selected to represent potential future pathways of greenhouse gas concentrations, aerosols and other atmospheric chemical constituents: medium (RCP4.5) and high (RCP8.5) emissions of greenhouse gases (RCP stands for 'representative concentration pathway') (Figure 1.2). The medium RCP4.5 scenario sees emissions peak by mid-century at around 50% higher than the 2000 level then rapidly decline over 30 years before stabilising at half of the 2000 level. The high RCP8.5 greenhouse gas emission scenario simulates rapid emission increases through early and middle parts of the century to reach 950 ppm CO_2 by 2100. Both RCP4.5 and RCP8.5 were the only RCPs available for a dynamically downscaled regional climate model over Australia.

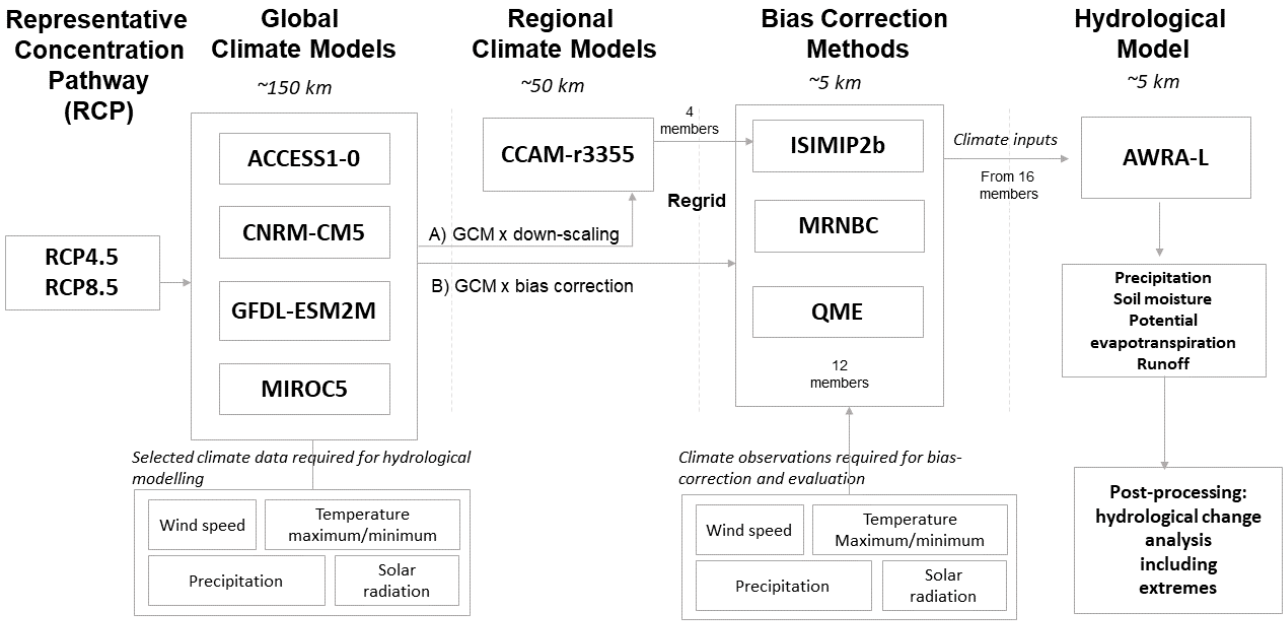

Figure 1.2. National Hydrological Projections showing details of the processing steps: i) 2 representative concentration pathways (RCP4.5 as medium and RCP8.5 as high) are selected, ii) 4 CMIP5 global climate models (GCMs) are selected, iii) path A – each GCM is downscaled by a regional climate model (RCM) to a 50km (0.5°) scale and then re-gridded to a 5 km (0.05°) scale. The RCM uses one bias-correction method (ISIMIP2b) that corrects the necessary climate inputs (precipitation, temperature, wind and solar radiation) against observations, iv) path B – each GCM is re-gridded to a 5 km (0.5°) scale and corrected directly using one of 3 bias-correction methods, and v) climate data from the 16-member ensemble is used to run the hydrological Australian Water Balance Model (AWRA-L) to produce hydroclimate change information for precipitation, soil moisture, runoff and evapotranspiration. These hydroclimatic variables are processed to understand future changes on the Australian water cycle components, including extremes

As shown in Figure 1.2, 4 CMIP5 GCMs were chosen, each with a spatial resolution of about 150 kilometres (km) (Srikanthan et al. 2022). These climate models were chosen as a subset of the models used in the Climate Change in Australia assessment (see Chapter 5 in CSIRO & Bureau of Meteorology 2015). The 4 global climate models were selected to represent a range (wet, medium and dry) of plausible future climates across Australia and for their ability to provide all the necessary climate inputs for the Australian Water Resources Assessment Landscape hydrological model (AWRA-L, version 6.1) (Frost & Wright 2018). In addition, a regional climate model (RCM) was used to bring each of the 4 selected GCMs to a finer resolution output of about 50 square kilometres (km^2) over Australia. These regional models better account for regional climatic influences, such as local topography.

Before using climate inputs from climate models, biases in the global and regional climate model forcing were corrected against observations in a process called bias correction. Three bias-correction methods were applied to the climate data from the models, resulting in the following 16-member ensemble (Figure 1.2):

- 12 members – comprising each of the 4 global climate models corrected with 3 different bias-correction methods
- 4 members – comprising each of 4 global climate models, downscaled and adjusted to a finer resolution as a regional climate model and corrected with one bias-correction method.

Each ensemble member reflects the chosen characteristics of its bias-correction method; the range of ensemble members lets decision-makers select the approach best suited to their needs.

To examine future impacts of climate change and to inform decisions on adaptation, outputs from the climate modelling process were re-gridded to a 5 km scale and used in our hydrological model to provide projections at that scale across Australia. Using bias-corrected climate inputs of precipitation, temperature, wind and solar radiation from the 16-member ensemble, the hydrological AWRA-L model produced daily model outputs over Australia of soil moisture, runoff and potential evapotranspiration (the amount of evaporation and transpiration that would occur at a particular location when water available for this process is non-limited).

To assess hydrological changes, temporal results are aggregated in 30-year periods centred around 2030, 2050, 2070 and 2085 on annual and seasonal timescales. These results are shown as maps demonstrating the spatial variability of the region’s change or as graphs showing aggregated results across the regions.

Each step of the National Hydrological Projections modelling chain is carefully evaluated to understand uncertainties associated with the modelling process. Uncertainties in hydroclimate change analysis can come from multiple sources, including:

- how greenhouse gas emissions will change into the future
- the processes represented in the climate models
- the effect of bias-correction and downscaling processes
- the hydrological modelling itself.

More details on how we address these uncertainties are discussed in Chapter 3. Further information on these models and the choices made in their selection as well as the evaluation process are detailed in our scientific publications and reports.

1.2 National Hydrological Projections hydrological assessment reports

Projection results feature many sources of uncertainty, including uncertainty over future trajectories of atmospheric greenhouse gas concentrations, how a warmer climate will lead to changes to hydroclimatic features and feedback loops, and the ability of climate models to represent those features. Acknowledging these uncertainties, the National Hydrological Projections ensemble provides a unique opportunity to examine impacts of plausible future changes on Australia's hydroclimate and its water resources.

To understand future impacts on Australia's water resources, region-specific assessment reports have been prepared on plausible future hydrological changes, including changes in precipitation, runoff, potential evapotranspiration and soil moisture as well as changes in extremes including droughts and floods. These assessment reports are based on 8 regions, formed from clusters of natural resource management (NRM) regions of Australia, that can be affected differently by climate change. These regions broadly represent groups of similar climatic and biophysical settings in Australia and corresponding natural resources. The National Hydrological Projections build on these regions and the scientific work that was previously carried out by the Climate Change in Australia (CCiA) initiative (CCiA n.d. a). CCiA provided the most nationally comprehensive, robust and consistent scientific information on future climate changes for Australia. Projected climate change has been described in detail in the individual CCiA reports for the NRM clusters (CCiA n.d. b), with additional regional detail being provided through ongoing initiatives from Australian state and federal governments. This work builds a complementary picture in the context of the regional hydrological cycle, regional water assets and its future impacts.

These hydrological assessment reports are a demonstration case of the applicability of the National Hydrological Projections data and plausible future water resource impact analysis across Australia. They are intended to provide a high-level regional picture and raise awareness of plausible hydrological changes for a water-sensitive audience, including Australia's water, energy and environmental managers; emergency and recovery services; transport operators; farmers; and people generally interested in future changes to water resources. The reports present information in the form of 'storylines' of plausible future occurrences of hydrological extreme events (e.g. floods) and long-term hydroclimatic changes. This information can be used to guide investment decisions and develop mitigation and adaptation strategies.

This report focuses on the Murray Basin region and is structured as follows:

- Chapter 1 introduces the National Hydrological Projections.
- Chapter 2 describes the assessment region, including its physiographic and hydroclimatic characteristics, recent conditions and long-term hydroclimatic trends.
- Chapter 3 evaluates our ability to simulate future hydrological changes, including the multiple levels of uncertainty, whether the climate models chosen can represent the region's climate and how well the hydrological AWRA-L model performs in the region. It also presents the results from the evaluation of the bias-correction methods. This information provides important context for the following chapter.
- Chapter 4 assesses the region's future hydroclimate conditions, which are presented as available National Hydrological Projections storylines. Changes are shown for precipitation, evapotranspiration, soil moisture and runoff assessed against the reference period (1976–2005). The chapter also provides insights into plausible future extremes of wet and dry periods.
- Chapter 5 demonstrates the applicability of storylines by exploring future water-sensitive impacts of selected case studies.

All foundational National Hydrological Projections datasets underpinning the assessment report analyses are also available as application-ready datasets via the National Computational Infrastructure (NCI) Data Catalogue (https://dx.doi.org/10.25914/6130680dc5a51).

For further detailed regional analysis, guidance on the use of National Hydrological Projections data or further general information, please contact us via water@bom.gov.au.

2 Regional description and hydroclimate of the Murray Basin region

The Murray Basin region incorporates the agriculturally productive lower reaches of the Murray–Darling Basin, Australia's largest basin covering an area of 459,000 km^2 (Figure 2.1). The Murray Basin region is known as Australia's food bowl, and its agricultural water use comprises approximately one-third of Australia's total water use (Bureau of Meteorology 2020). The headwater catchments of the Murray River border the eastern edge of the region along the Great Dividing Range. The Murray Basin region includes several main rivers originating in the Australian Alps, including the Mitta Mitta, Kiewa, Goulburn, Ovens and Broken rivers, and the Murrumbidgee River joins the Murray River south-west of Balranald. The Loddon and Avoca rivers have their headwaters in the Central Highlands of Victoria.

The Murray River meanders along a total distance of 2,500 km north-westerly across the Australian inland plains of New South Wales and Victoria. Waters from the Murray and the Darling rivers join in Wentworth just west of Mildura before reaching the ocean in the Coorong – an extensive saline lagoon on the coast of south-east South Australia. The western boundary of the Murray Basin region includes the lower part of the Flinders ranges.

Figure 2.1 Murray Basin region

The largest population centre within the region is Canberra, although there are also several important regional centres in the area including Bendigo (Figure 2.1). This region encompasses 17 surface water storages (>100.000 ML) including some of the largest storages in Australia (see Figure 2.1 and section 2.3) that supply water to cities and towns within and outside the region.

The Murray Basin region supports a range of water-dependent industries, including cropping and intensive agriculture, water security for urban supply, hydropower and alpine tourism. Natural, water-dependent assets in this region include internationally recognised Ramsar wetlands and other important aquatic ecosystems including iconic wetlands such as the Coorong or Murray Mouth as well as large floodplain forests of river red gums and a wide variety of native plant and animal species and migratory waterbirds.

2.1 Climate

Generally, summers in the Murray Basin region are warm and winters are mild, with an annual mean temperature gradient from 18 ˚C on average in the hot and dry grasslands in the north-west and 12 ˚C on average further south

and east. High-altitude areas including along the Great Dividing Range experience mild summers and can see snowfall during winter months, with annual mean temperatures as low as 5 °C. Decreases in snowfall amount and extent in alpine regions have been observed since the 1950s and are expected to continue with rising temperatures.

Weather and climate variability in the Murray Basin region is predominantly influenced by the seasonal position of the sub-tropical ridge (STR), a climatological band of high-pressure systems characterised by relatively dry air and often little precipitation (see Figure 2.2) (Pepler et al. 2018; Timbal et al. 2015). The STR divides the northern areas influenced by the tropics from the southern areas influenced by westerly winds and winter precipitation. Rain-bearing cold fronts and low-pressure systems from the Southern Ocean bring precipitation to the Murray Basin region when the STR is at its most northerly position. This occurs during the winter months when the temperature gradient between the warm equatorial regions and the cooler southern regions is smallest (Drosdowsky 2005; Pepler et al. 2018). Precipitation over the Murray Basin region is also associated with cut-off lows (Pepler et al. 2020), upper-level disturbances (Reid et al. 2019, Risbey et al. 2009) and thunderstorms (Dowdy 2020). When these systems occur together (for example, a low with embedded thunderstorms), the resultant precipitation can be very heavy (Dowdy & Catto 2017; Pepler et al. 2020).

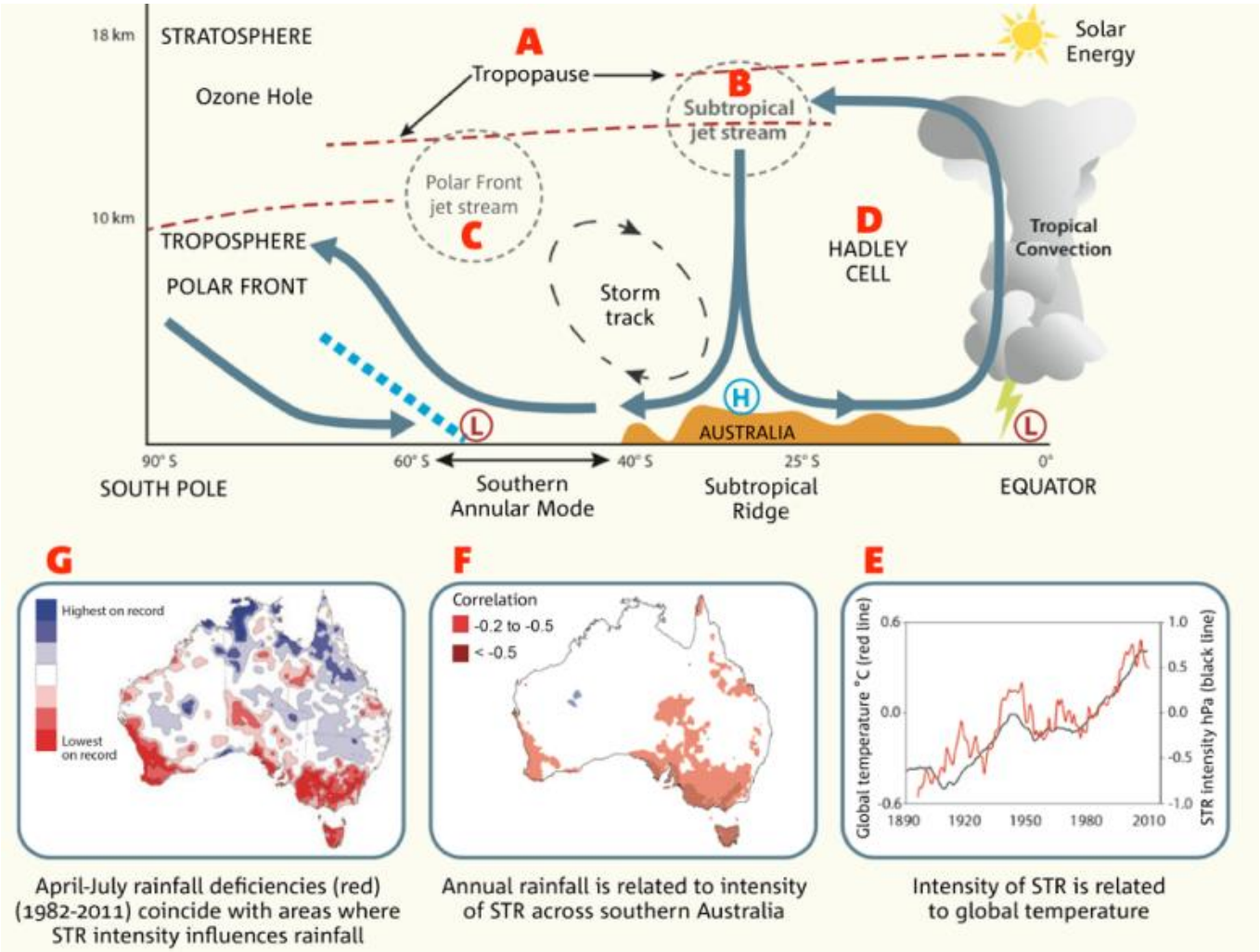

Figure 2.2. Observed changes in average circulation from the tropics to the pole and their relevance to Murray Basin precipitation (source: Timbal et al. 2015). See the location of the subtropical ridge over Murray Basin region in the top panel. Precipitation deficiencies in recent decades (G), coincide with locations where there is the greatest link between the intensity of the sub-tropical ridge and precipitation (F). As the pressure has increased in the sub-tropical ridge, the global temperature has also increased (E)

The average annual precipitation varies from about 200 mm in the western part of the Murray Basin to over 1,200 mm in the mountainous region in the south-east and east of the basin (Figure 2.3a). A similar pattern is observed for the runoff (Figure 2.3b) and soil moisture (Figure 2.3d) while the potential evapotranspiration decreases in a north–south direction (Figure 2.3d). Snow occurrence in the alpine regions of the Great Dividing Range during the winter months can lead to some delay in the timing of runoff.

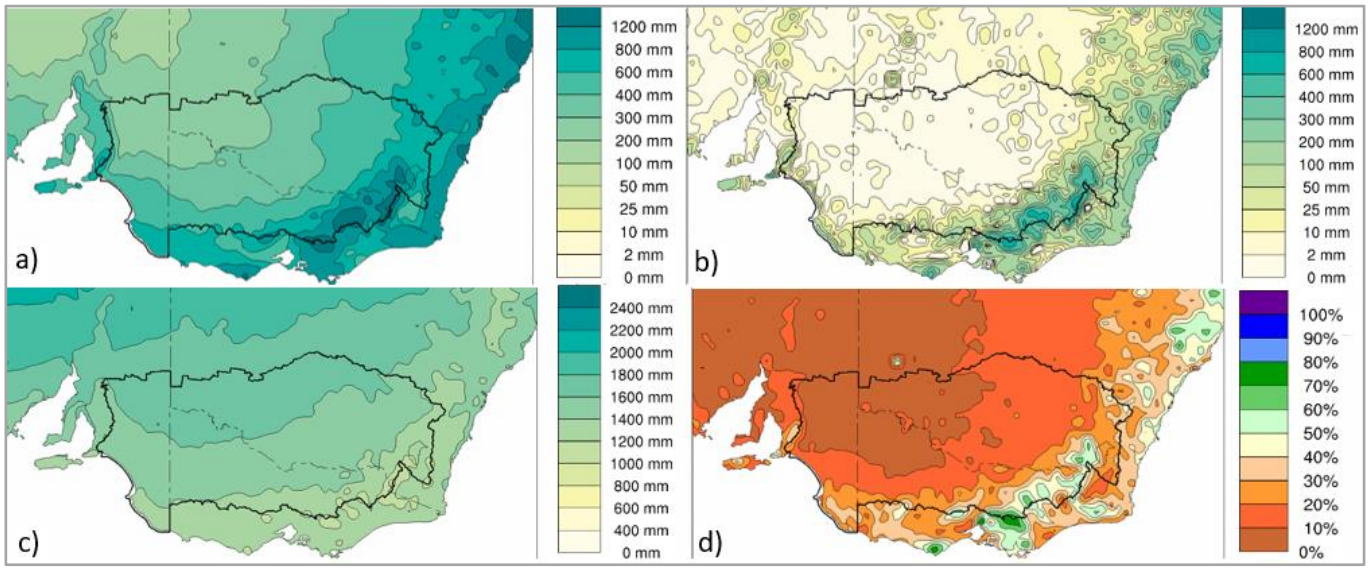

Figure 2.3. Murray Basin annual average hydroclimate (1976–2005) showing (a) observed precipitation and AWRA-L modelled values for (b) runoff, (c) potential evapotranspiration and (d) soil moisture

Precipitation and temperature are linked in the region, with heavy rain events leading to cooler daytime temperatures that can persist for months due to increased volumes of soil moisture (Hope & Watterson 2018). Night-time minimum temperatures can be warmer than average during the periods of heavy rain, but cooler nights have been observed during subsequent months due to the influence from wet soils. Clear, cloud-free winter skies, associated with a strong STR and the prevalence of high-pressure systems, can lead to cool nights during the winter months (Pepler et al. 2018). However, clear skies in other seasons are associated with warm night-time temperatures, and warm days in all seasons.

Droughts and floods are a common feature of inland eastern Australia and the Murray Basin region. While precipitation is brought by the range of weather systems described above, the prevalence of these can be influenced by large-scale natural modes of variability of the climate system including the El Niño–Southern Oscillation (ENSO) and the Indian Ocean Dipole (IOD). Crucially, year-to-year variability and multi-year variability are large, with dry years and long dry periods interspersed with wet and very wet years. There is, however, a marked annual cycle in the variability with most of the precipitation to occur during the months from July–October (Figure 2.4). Cool-season precipitation is generally more reliable than warm-season precipitation, which can vary substantially. Monthly potential evapotranspiration follows the temporal pattern of temperature (Figure 2.4) and is the lowest during June–July with less than 50 mm/months during this period (Figure 2.5).

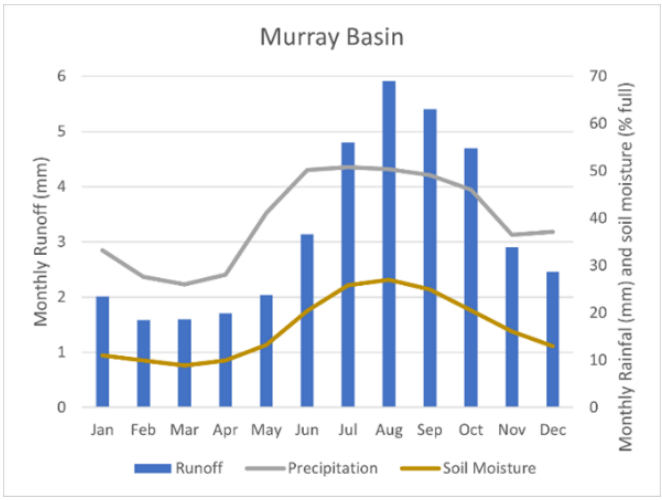

Figure 2.4. Monthly average observed precipitation and AWRA-L modelled runoff and soil moisture for the Murray Basin region for the reference period (1976–2005)

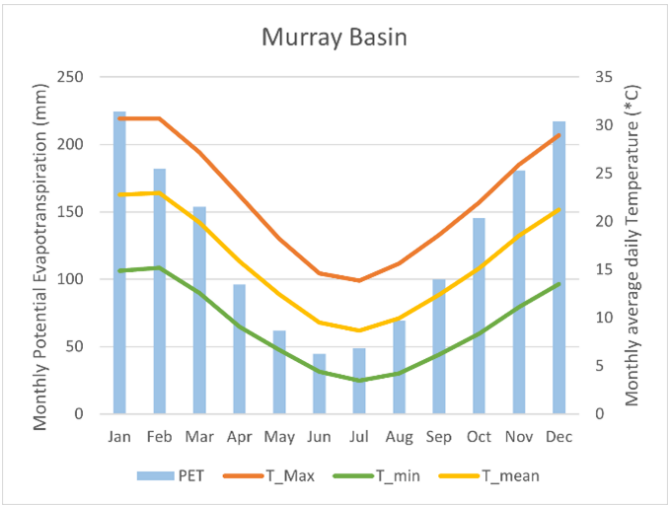

Figure 2.5 Monthly average observed temperature and AWRA-L modelled potential evapotranspiration for the Murray Basin region for the reference period (1976–2005)

Most surface water runoff in the Murray Basin region is generated in the mountainous, alpine regions, where average annual precipitation ranges mostly between 1,200 mm and 1,800 mm, and a few areas exceed 2,400 mm. This equates to average runoff values of from 400 mm to more than 800 mm in the alpine areas. Precipitation in alpine regions is dominant during the cool season, most falling from June to September or October. Combined with low temperatures, low potential evapotranspiration rates and soil moisture filling up depleted moisture stores, the cool season dominates runoff generation in this region and is the main infilling period for storages.

Average annual precipitation in the flat inland areas of the region typically ranges from 400 mm in the east to less than 50 mm in the west. Due to high evapotranspiration rates, most of these inland areas experience less than 5 mm annual runoff. Water consumption in these flatlands is dominated by groundwater with aquifers largely consisting of sedimentary and alluvial deposits. A substantial volume of groundwater enters the rivers in the upper and middle catchments as baseflow and then re-enters the groundwater systems further down through seepage from streambeds. Groundwater recharge in the flat areas is typically low. It is only elevated once overbank flows occur during flooding. As most of the western part of the Murray Basin region lies on flat plains that are not far above sea level, the rivers in these areas tend to flow slowly. Some rivers, like those in the Wimmera, even end up in wetlands.

2.2 Recent hydroclimatic trends and condition

The interplay of the various climate drivers leads to high year-to-year variability in precipitation, temperature, soil moisture and runoff across the region (Figure 2.6). Runoff and soil moisture show a decreasing trend in the recent past while potential evapotranspiration shows a slight increase associated with observed increases in temperatures.

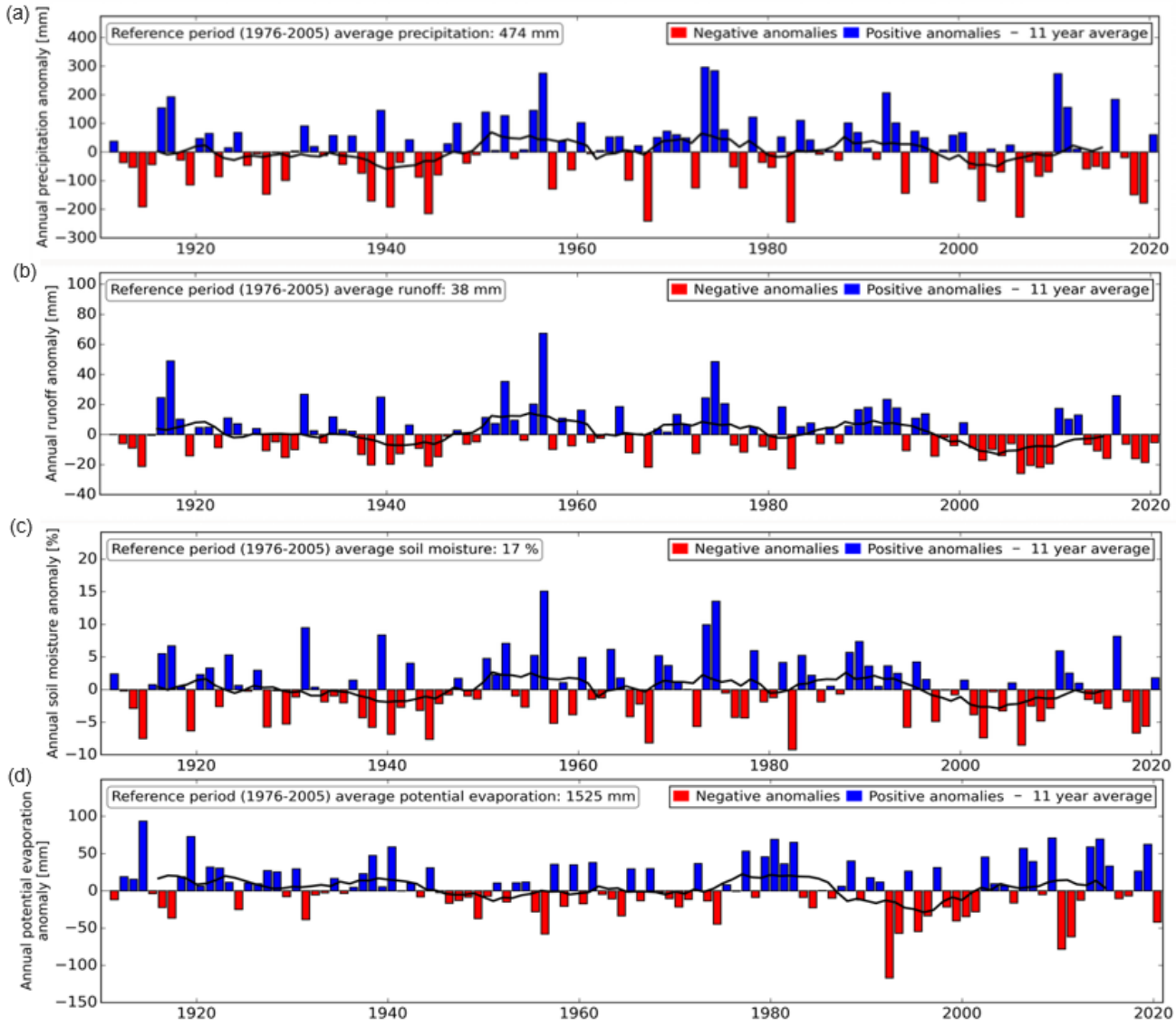

Figure 2.6. Murray Basin annual anomalies relative to the reference period (1976–2005) mean in (a) observed precipitation and AWRA-L modelled values for (b) runoff, (c) soil moisture and (d) potential evapotranspiration

The last 20 years in the Murray Basin region has included the record-breaking Millennium drought (2001 to 2009), which affected most of the Murray–Darling Basin, and 2 of the wettest years on record for Australia (2010 and 2011), which ended the drought. The Millennium drought was dominated by a strong decline in winter precipitation, which continued through the very wet La Niña years of 2010 to 2011. Within the past 20 years, only 4 years showed above-average hydroclimatic conditions, indicating a recent drying trend for the region. This aligns with findings from Wasko et al. (2021) on streamflow trends. They found decreasing streamflow trends since 1970 in all 53 observation sites within the region.

2.3 Water availability and management

Water resources of the River Murray are highly regulated. Resources are allocated to provide water for a range of purposes including hydro-electric power generation, urban centres, irrigated agriculture and the environment, throughout the entire river valley and beyond. There are major water storages in the region that are predominantly located along the alpine ranges in the south-east of the catchment (Figure 2.1). Storages fill from high-altitude headwater catchments that are generated by annual runoff volumes that are the highest in this region. Some of the surface water generated in this area is diverted from the headwaters of the Snowy River via Lake Eucumbene westward through the Great Dividing Range and released into the Murray River catchment.

The region includes some of Australia's largest water storages: Lake Hume, Dartmouth, Burrinjuck, Lake Eildon and Blowering (Figure 2.1), with a combined total accessible capacity of about 12,880 GL. Water fills these storages primarily during the winter months. In conjunction with licensed streamflow abstractions, and to a lesser degree groundwater abstraction, these storages provide water to support human consumption (including Canberra, with a population of over 400,000 people), environmental flows and agricultural use. The water resources are managed by a network of stakeholders including federal government policymakers, and environmental water holders, state government allocation and entitle managers, water managers, river operators and private irrigation companies that organise water transfers on behalf of irrigators. Water in the River Murray is shared based on the rules set out in the Murray–Darling Basin Agreement.

This highly managed and transferred system means that water that first enters a stream high in the alps may be used for irrigation in the town of Hay many hundreds of kilometres away. The key demand period for these water sources is over the warmer months to meet irrigated water needs. This heavily engineered environment supports a complex management system that includes significant inter-valley transfers to optimise hydro-electricity generation and also trading and agricultural demand. A complex entitlement and allocation system is a significant factor affecting sub-annual and inter-annual storage volumes and streamflow. That is, seasonal hydrological patterns in many parts of the catchment are strongly influenced by river operations that can change natural streamflow cycles and fluctuations. The only sources of water that are directly connected to climate fluctuations are supplementary flows. These are licensed but unallocated flows that are authorised by river managers during certain periods of high flows.

The Ovens River and adjacent Kiewa River in the south-east of the region are the only largely unregulated rivers of the Murray Basin, providing a natural flow regime for a relatively small portion of the region. Outside the unregulated catchments, environmental flows requirements are an important water management factor, and they interact with the entitlement structures and river operations of the system. Environmental watering also requires flood plain inundation, and there are specific challenges with implementing successful environmental watering programs and optimising these against other beneficial uses.

3 Ability to simulate hydroclimatic conditions of the Murray Basin region

Assessing how well climate and hydrological models simulate key elements of the hydroclimate for Australia and the Murray Basin region is an essential part of understanding the potential future impacts of climate change. Assessments of model performance against observations and the latest scientific understanding of hydroclimatic processes provide a basis for confidence, in the sense of enabling trust in sets of projections. Models are not expected to reproduce observations exactly but rather are assessed in terms of their ability to capture important aspects of variability and their representation of important processes. Bias correction is an important step in the process of hydrological impact modelling. It brings information simulated by global climate models about the impacts on our climate system of rising greenhouse gases together with our best representation of hydrological processes at local scales (in this case, the assessment region). Bias-corrected climate data and the simulated hydrological output data are compared against observations to assess the performance of the models and processes. For a detailed description of the modelling process and a technical assessment of performance, please see the National Hydrological Projections technical report (Srikanthan et al. 2022).

Climate and hydrological models are always an imperfect representation of the reality (and plausible future) and are therefore associated with various sources of uncertainties. These uncertainties are intrinsic to hydroclimatic modelling and arise from the selection of climate models and the differences in model responses in a warming climate. These differences include the representation of climate drivers and their expression through, for example, El Niño and La Niña events and can also include the uncertainty of future human behaviours affecting greenhouse gas emissions. Further sources of uncertainties stem from the influence of bias corrections as well as from the hydrological modelling and the representation of hydrological processes itself. Thus, we can never forecast the exact time series of Australian temperature, precipitation and other climate drivers, and the National Hydrological Projections will differ from observations over short to medium periods. These uncertainties influence our ability to simulate the hydroclimate in Australia. This section briefly introduces the models and methods used in these National Hydrological Projections and assesses our ability to simulate the hydroclimate of the Murray Basin in the context of uncertainties. More details on the methods used can be found in the technical report (Srikanthan et al. 2022).

A number of choices were made in developing the datasets used in these National Hydrological Projections. Four global climate models (GCMs) were selected: ACCESS1-0, CNRM-CM5, GFDL-ESM2M and MIROC5. These models were selected from the suite of 42 models in the international Coupled Model Intercomparison Project Phase 5 (CMIP5). These 4 were chosen because they fulfilled important requirements, including the following:

- GCM data was available for input into the hydrological models.
- The GCM had been used to force one or more dynamical downscaling models.
- The GCM represents the large-scale drivers of climate and weather variability well.
- The GCM simulates Australia's precipitation, temperature, wind and radiation relatively well.
- The 4 models together represent the range of future precipitation and temperature changes relative to the spread of the 42 models of the CMIP5 ensemble.

The range of climate responses from each GCM, in any particular year, derives from the particular state of the weather and large-scale variability occurring within that model in that year. Each GCM models its own weather, and the climate varies over the longer term of the simulation in response to changing atmospheric levels of greenhouse gases, aerosols and ozone in the upper atmosphere (and the Antarctic ozone hole).

In addition, one atmosphere-only climate model was used to 'downscale' the GCMs from their 150 km resolution to 50 km. CCAM, CSIRO's Conformal Cubic Atmospheric Model, is a global model in which the grid point spacing is stretched to have fine resolution over Australia. Additional dynamically downscaled data was available to the National Hydrological Projections under the Victorian Climate and Water Initiative (VicWACI) and other initiatives of the Victorian Government. Another regional model known as WRF (Weather Research and Forecasting model)

dynamically downscaled the GCMs to about 50 km through the New South Wales Government–led partnership NARCliM (NSW and ACT Regional Climate Modelling). NARCliM output was included in the historical era simulations using the hydrological model but was not available for projections at the time of the release. The aim is to include further downscaling models in future updates to the projections service.

Three bias-correction methods were implemented to improve the representation of local climate conditions and reduce biases relative to observed data. First, the output of the GCMs and downscaling model were scaled down from their original scale (about 150 × 150 km) to 5 × 5 km resolution using a conservative re-gridding method; then the bias correction was applied. Each of the bias-correction methods is designed to preserve various features of the climate signal such as trend, inter-annual variability or seasonality of a climate variable.

The ability of each ensemble member to simulate the future hydroclimate of the Murray Basin region was assessed by evaluating its ability to reproduce the observations and observation-based model results of the 1976 to 2005 reference period. This evaluation let us identify any biases in the models that were likely to be carried forward into future projections. A range of evaluation techniques and statistics were used to evaluate the ability of the ensemble to simulate the hydroclimate of each individual region.

The following 3 bias-correction methods were used:

- ISIMIP2b, a quantile-based method that preserves the trend in the data (Hempel et al. 2013)
- QME, a quantile-based method that models the extremes well (Dowdy 2020)
- MRNBC, a method that preserves the interdependence among the variables as well the low-frequency characteristics (Johnson & Sharma 2012; Mehrotra & Sharma 2016).

The bias-corrected data was evaluated to assess the effectiveness of the bias-correction methods. The AWRA-L model (see Section 3.2) was then run with the bias-corrected climate data as input.

3.1 Ability to simulate the key climate drivers

The skill of the 4 National Hydrological Projections GCMs (among other GCMs) to represent the key large-scale drivers of Australia's climate was assessed previously by the Climate Change in Australia initiative (Moise et al. 2015). This assessment provided a basis for placing confidence in the model's projection for Australia and identified individual ensemble members or ensemble groups that may have significant performance issues in simulating a key aspect of climate variability.

Many CMIP5 GCMs have a bias in the Pacific Ocean whereby the ENSO signal extends too far towards Australia along the equator (Grose et. 2017). This bias is minimal in the 4 National Hydrological Projections models selected; thus they represent the processes influencing climate variability in northern and eastern Australia reasonably well (Brown et al. 2016). A common bias seen in the eastern Indian Ocean in the Australian spring is relatively small in 3 of the models. However, CNRM-CM5 has this bias, which might limit the expected increase in the frequency of extreme positive Indian Ocean Dipole events and their expression through dry conditions in south-east Australia (Wang et al. 2017).

The 4 GCMs chosen for these projections, ACCESS1-0, CNRM-CM5, MIROC5 and GFDL-ESM2M (Table 3.1), were found to represent the weather-scale features influencing northern Australia well, and their future changes should be considered reliable. However, CMIP5 GCMs in general do not capture the eastward propagating sub-seasonal monsoon activity, cloudiness and precipitation linked to the Madden–Julian Oscillation (Moise et al. 2015).

Table 3.1. Details of selected global climate models

Climate model	Type	Institute	Country of origin	Reference
ACCESS1-0	Global	CSIRO and Bureau of Meteorology	Australia	Collier and Uhe (2012)
CNRM-CM5	Global	Centre National de Recherches Météorologiques – Groupe d'études de l'Atmosphère Météorologique (CNRM-GAME) and Centre Européen de Recherche et de Formation Avancée	France	Voldoire et al. (2013)
GFDL-ESM2M	Global	Geophysical Fluid Dynamics Laboratory, National Oceanic and Atmospheric Administration (NOAA)	USA	Dunne et al. (2012)
MIROC5	Global	Japan Agency for Marine-Earth Science and Technology (JAMSTEC)	Japan	Watanabe et al. (2010)
CCAM r3355	Regional	CSIRO	Australia	Rafter et al. (2019)

MIROC5 fulfils the requirements for inclusion in our ensemble although it does not represent the weather features that are important for the southern Australian climate as well as some others and might be considered less reliable. However, its inclusion helps the National Hydrological Projections GCM ensemble embrace the range indicated by the full range of 42 CMIP5 models (Srikanthan et al. 2022).

3.2 Hydrological modelling: the Australian Water Resources Assessment Landscape model (AWRA-L)

The Bureau's operational Australian Water Resources Assessment Landscape model (hereafter AWRA-L) was used to project root zone soil moisture, potential evapotranspiration and runoff. AWRA-L is a daily semi-distributed water balance model based on a 5 × 5 km (0.05°) grid. It models hydrological processes separately for each spatial unit, called a hydrologic response unit (HRU). At each grid cell it simulates the flow of water through the landscape: precipitation entering the grid cell, passing through the vegetation and soil moisture stores, and leaving the grid cell through evapotranspiration, runoff or deep drainage to the groundwater (Figure 3.1). Each grid cell in AWRA-L is divided into 2 HRUs, these represent deep-rooted vegetation (trees) and shallow-rooted vegetation (grass). The spatial distribution of the HRUs remains static over time and does not reflect land use change.

The AWRA-L model is calibrated at the national scale to match streamflow, soil moisture and evapotranspiration observations from across the country. This calibration enables a nationally consistent dataset, but model evaluation results can vary between regions and landscape features (Frost & Wright 2018).

Model performance can be affected by the number of calibration catchments local to the region or representative of the landscape feature. AWRA-L better captures the runoff dynamics in wetter regions and periods, while discontinuous runoff regimes, consisting of long dry periods followed by short periods of extreme precipitation, are more difficult to characterise. A positive bias in runoff can result in areas with extended periods of no flows in central and northern Australia. Groundwater–surface water interactions are not well represented in AWRA-L, resulting in a drop in performance in areas where there is a high dependency on the contribution of baseflow to the generation of streamflow.

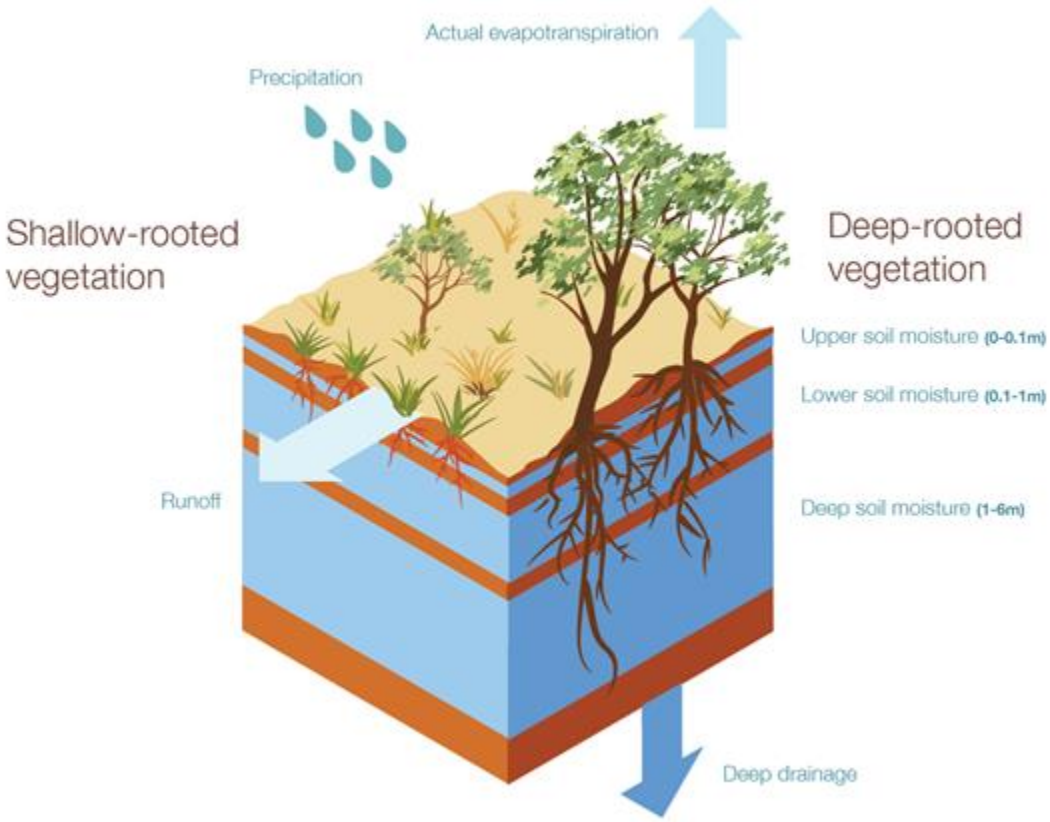

Figure 3.1. AWRA-L model grid cell with key water stores, fluxes and the hydrologic response units of deep- and shallow-rooted vegetation

The Bureau's operational AWRA-L was chosen as the hydrological model based on the evaluation and benchmarking of the available national models presented in Frost & Wright (2018). Importantly, this evaluation considered runoff, soil moisture and actual evapotranspiration in the assessment of the models. AWRA-L was run independently using the bias-corrected GCM climate data as input. The lack of feedback between the GCMs and AWRA-L means that the potential role of increased carbon dioxide levels on vegetation growth and evapotranspiration rates are not modelled (Greve et al. 2017; Yang et al. 2019). Future land use changes and vegetation changes resulting from future temperature and water availability changes are also not considered in AWRA-L or the GCMs. Together these factors will grow in importance over time, adding an extra facet of uncertainty to the soil moisture and runoff projections later in the century. A detailed description of the quantification of the AWRA-L model uncertainty can be found in Azarnivand et al. (2022).

3.3 Ability to simulate the hydroclimate of the Murray Basin region

The 4 GCMs were chosen to represent the range of future precipitation and temperature changes for Australia as described in the National Hydrological Projections technical report (Srikanthan et al. 2022). The 4 selected GCMs were compared to the entire ensemble of 42 CMIP5 Climate Change in Australia (CCiA) models to see how these models represent wet or dry futures (Figure 3.2). This provides an overview of how the selected GCMs rank relative to the full CMIP5 ensemble across Australia and respective climate variables.

The 4 global climate models chosen for these projections, ACCESS1-0, CNRM-CM5, MIROC5 and GFDL-ESM2M (Table 3.1), were found to represent Australia's weather-scale features well, and their future changes should be considered reliable (Grose et al. 2015). In the Murray Basin region, the 4 GCMs capture the central range of change in precipitation for mid-century (2030), with the wettest and driest scenarios omitted. For late century (2070), the GCMs include examples of both the wetter and drier extremes. The full CMIP5 ensemble of 42 models projects an increase in temperature in the Murray Basin region, and the selected 4 capture the central to lower end of this range. Overall, the 4 GCMs are representative of the projected future climate in the Murray Basin region

with a tendency towards moderate precipitation scenario, missing some of the extreme wet and extreme dry simulations, and not as much warming as the full suite of CMIP5 GCMs.

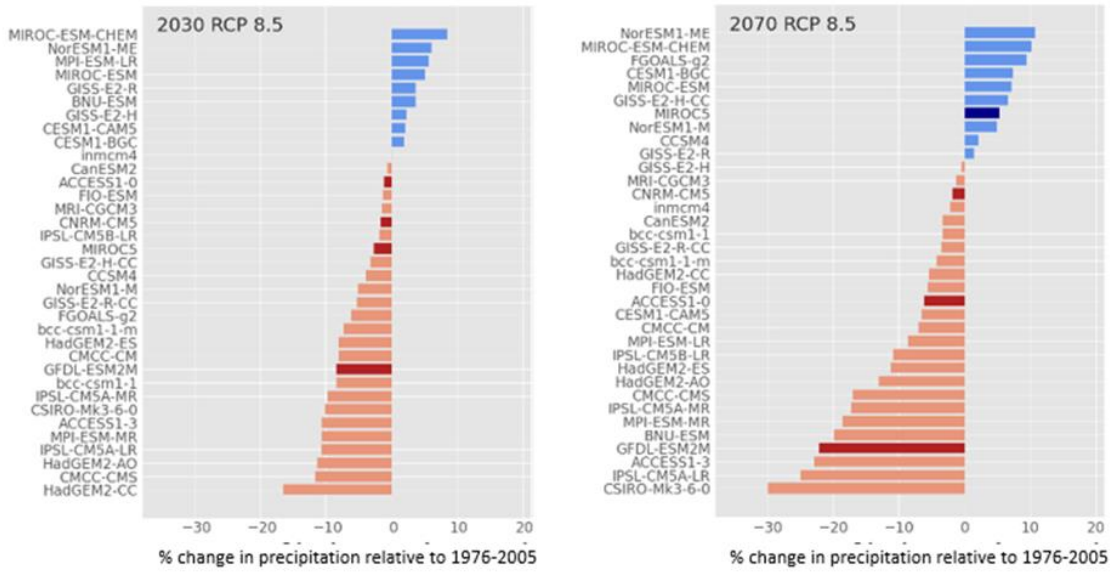

Figure 3.2. Ranking of the Murray Basin region precipitation projections for the GCMs used in this study (shown in darker colours) compared to the CCiA ensemble for RCP8.5 for (a) 2030 and (b) 2070. The horizontal bars indicate the change signal – the difference of the regional average quantity from the monthly pattern for the reference period (1976–2005)

Simulated hydroclimate data for the current climate (produced by the 16-member ensemble) is assessed by comparing it with observational datasets from AWAP (Jones et al. 2009). In addition, 3 outputs (soil moisture, runoff and potential evapotranspiration) obtained by forcing the AWRA-L model with AWAP and bias-corrected data were also compared. Since the models are not perfect representations of the world, the simulated data will not exactly match the observed data. A certain tolerance level is used in assessing the model simulations.

The evaluation of the ability of the ensemble members to replicate the reference period (1976–2005) observations and model runs revealed overall minimal bias in the Murray Basin region. The precipitation and temperature observation networks are relative sparsely distributed across the western, inland parts of the Murray Basin region. This introduces some uncertainty into the baseline climatology, but there is good coverage along the south and south-east. As the GCM climate data is bias corrected to the historical gridded data, these anomalies translate into the projections.

Evaluation criteria, such as representing the seasonality of the climate variables, are found to be adequately preserved in all ensemble members with suitable results for temperature, windspeed and potential evaporation. There are some seasonal precipitation biases for individual ensembles or ensemble groups including a negative bias of about 6% for summer ensemble members bias-corrected with MRNBC. In general, there are no significant biases in the other ensemble member groups. Additionally, there is a general negative bias in most cases for mean annual and seasonal solar radiation; however, this bias is relatively small with the largest bias around 1.5% (see Appendix Figures 8.1 to 8.10). From the above discussion, it can be concluded that the bias-correction methods successfully corrected the GCM data except for one case of precipitation. However, QME did not preserve the climatology for precipitation.

Biases in the hydrological variables, including potential evapotranspiration, soil moisture and runoff, are calculated by comparing the results produced by the ARWA-L model forced with observed climate inputs and those modelled by the ensemble for the 1976 to 2005 reference period (for details see Appendix Figures 8.11 to 8.16). There is a relatively large spread of bias (up to 20%) for runoff in the Murray Basin region. Even though the climate data have

been successfully bias corrected, the larger bias in runoff might be due to the sequencing of the bias-corrected climate data, which could also cause the bias-correction methods not to preserve the climatology well.

The vegetation of the Murray Basin is dominated by agricultural lands, shrubs, heath and grasslands and is characterised by the shallow-rooted hydrological response unit in the AWRA-L model as well as alpine forests represented by deep-rooted vegetation (Frost & Wright 2018). There are some arid inland areas dominated by rock and impermeable surface that are not modelled in AWRA-L version 6.1 but will be in version 7. AWRA-L is a nationally calibrated model, and 53 of the 305 calibration catchments are in the Murray Basin region. The performance of the continentally calibrated AWRA-L model for the Murray Basin region is satisfactory based on the median monthly Nash–Sutcliffe coefficient of efficiency (NSE) (Nash & Sutcliffe 1970) greater than 0.6. Wasko and Nathan (2019) analysed streamflow trends post 1970 for both streamflow observations and modelled runoff from the AWRA-L model. They found that AWRA-L was able to match the trend direction of most of the 53 streamflow observation sites. AWRA-L correctly modelled increasing trend direction for 100% of sites for annual streamflow volumes, importantly 100% for winter volumes and 77% for summer volumes.

In summary, the ability of the National Hydrological Projections 16-member ensemble to simulate the hydroclimate for the Murray Basin is satisfactory. The evaluation shows a good ability to replicate climate data and identifies no significant bias in the hydrological model outputs, except for runoff.

4 Available National Hydrological Projections storylines for the Murray Basin region

Generally, projections provide a collection of plausible future 'storylines' rather than a forecast or likelihood of a specific outcome. Individually each ensemble member represents an internally consistent future storyline. Thus, while the ensemble members are based on slightly different physics, they all are built on plausible representations of physical processes. Individual ensemble members are the most appropriate method to represent this internal consistency and are a key element of establishing a storyline. No 2 ensemble members will follow the same changes in the many different climate features that can be considered.

The National Hydrological Projections used in this report allow for a unique region-wide assessment of projected hydroclimatic changes of the Murray Basin region. Results below are drawn from the assessment of the 16-member ensemble of hydroclimatic variables. The projected hydroclimate for the region is presented in this chapter as a set of available plausible future changes of key hydrological variables or storylines. It presents a set of key figures representing the change in the hydroclimate into the future under 2 different representative concentration pathways and showing how this change varies within the Murray Basin region.

In addition to the National Hydrological Projections, previous climate projections for the region are described in the Murray Basin CCiA report (Timbal et al. 2015). Some state-based datasets provide further projections information in parts of this region. For NSW, NARCliM provides detailed downscaled information at 10 km resolution (based on the previous generation of climate models, CMIP3) and the A2 projection scenario (similar to RCP8.5) (Adapt NSW n.d.). For the South Australian portion of the Murray Basin region, NRM region projections are presented by the Goyder Institute for Water Research (n.d.). For Victoria, results from the Victorian Water and Climate Initiative (VicWaCI) (DELWP n.d.) are described in DELWP et al. (2020), Hope et al. (2017) and South Eastern Australian Climate Initiative (SEACI n.d.). VicWaCI focuses on supporting the planning of water resource and flood managers. Victorian water resource managers are supported with guidelines for assessing the impact of climate change on water availability in Victoria (DELWP 2016, 2020). Victorian Climate Projections 2019 (VCP19) was an initiative based on 6 dynamically downscaled projections. Results are presented on the CCiA website (CCiA 2020). The dataset is similar to the projections from the GCMs combined with CCAM that are presented here. However, subsequent analysis procedures differ: VCP19 has a further downscaling step to 5 km whereas the hydrological projections ensemble used here is bias corrected. Together, there are at least 3 regional sources of climate projections information for the Murray Basin region. The National Hydrological Projections allow for a unique region-wide map of the historical and projected changes in the hydroclimate across the region.

4.1 Interpreting the National Hydrological Projections storylines

The projected future conditions are represented by the degree of change relative to the conditions of the reference period (1976–2005). Each of the 16-member ensemble is run for this reference period and for the future. As described in Chapter 3, each ensemble member is evaluated on the basis of the differences between the modelled reference period and the observations. These differences inform our assessment of the change in conditions projected by each ensemble member for the future. The change can be presented in absolute values (e.g. millimetres of precipitation) or as a relative proportion of the mean for the region (e.g. a 10% increase in precipitation). There is significant value in interpreting both absolute and relative values depending on the application.

Chapter 3 outlines how an ensemble of GCMs and bias-correction methods has been used to develop a range of plausible future conditions. This spread in the 16-member ensemble represents a range of plausible future conditions that decision-makers can use to explore impacts. The median of the 16-member ensemble represents a mid-range view of those plausible futures. The results are communicated against a series of future 30-year periods, which are referred to by their midpoint. For example, the results reported against 2050 represent the average of the 2036–2065 period. This allows us to identify general trends into the future beyond annual

fluctuations. Results from other projections are discussed to contextualise where these storylines fit in a broader understanding of plausible futures.

Spatial variations in the projected conditions are represented by the differences in ensemble median and only presented for the futures, representative concentration pathways and units that are most relevant to the key finding in the region. Inter-annual variability is visually represented by a single ensemble member (ACCESS1-0_ISIMIP2b) in the time series graphs. This single ensemble member time series should not be interpreted as a forecast for individual years; it is designed to model the extent to which the shorter-term climate drivers are likely to vary from the annual values.

Summary tables present key findings from multiple levels of evidence: projected results that describes the spread of the 16-member ensemble, concordance with historical trends reached by previous studies if available, and the assessment of the ability of the ensemble to simulate the hydroclimate in the region.

4.2 Precipitation

A time series of annual precipitation for the Murray Basin region from the 16-member ensemble is shown in Figure 4.1. The example model (ACCESS1-0_ISIMIP2b) output shown over the projections illustrates that this large year-to-year variability is projected to remain as a future key climate feature into the late century. Towards the end of the century there is a large spread among the 16-member ensemble where both drier and wetter futures are plausible due to variation in climate model sensitivity to increased greenhouse gas forcing.

Mean annual precipitation is projected to have a large ensemble spread with both increases and decreases plausible for all future time periods and both representative concentration pathways. By late century, the 16-member ensemble median projects a decreasing trend for RCP8.5. However, as the ensemble members project widely varying changes in annual precipitation, it makes the ensemble median a less reliable indicator of the change signal.

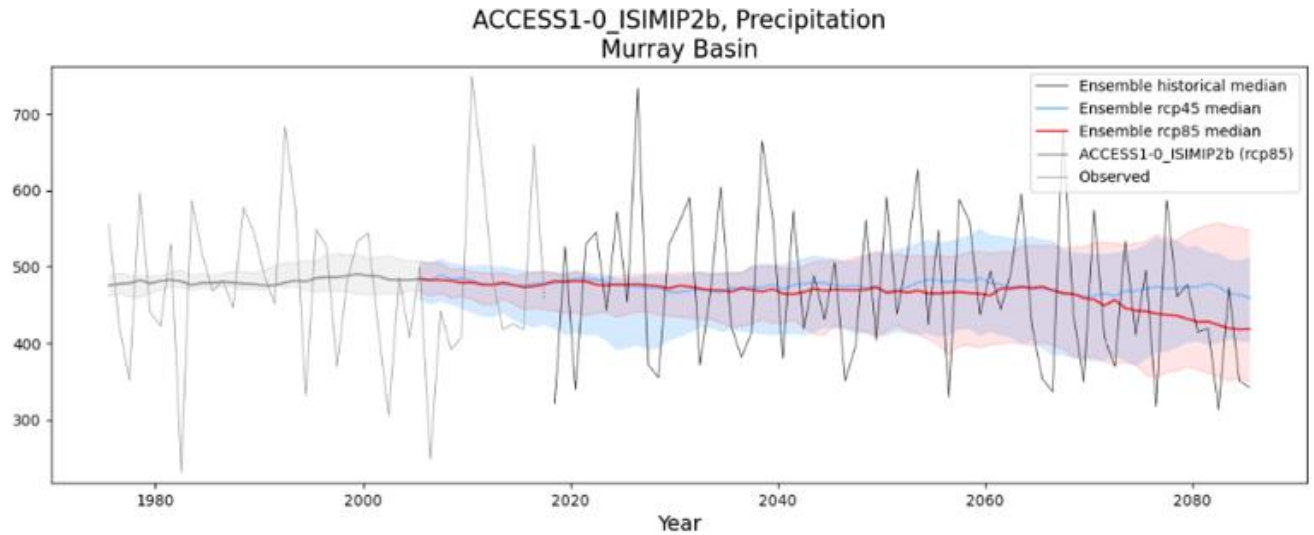

Figure 4.1. Annual modelled precipitation projected to 2099 by the 16-member ensemble for RCP4.5 (blue) and RCP8.5 (red) in the Murray Basin region. The shaded areas represent the 10th to 90th percentile range for all ensemble members in the historical and future time periods. The time series for ACCESS1-0_ISIMIP2b (RCP8.5) is included (dotted line) to show the variability projected for an individual ensemble member. The grey line represents the observed historical median precipitation based on AWAP data

While the median for annual precipitation under RCP4.5 projects little change, the median under RCP8.5 departs from this pattern by about mid-century, by which time almost all ensemble members project precipitation

decreases; the only projections for increased precipitation are associated with the generally wetter MIROC5 GCM (Figure 4.2).

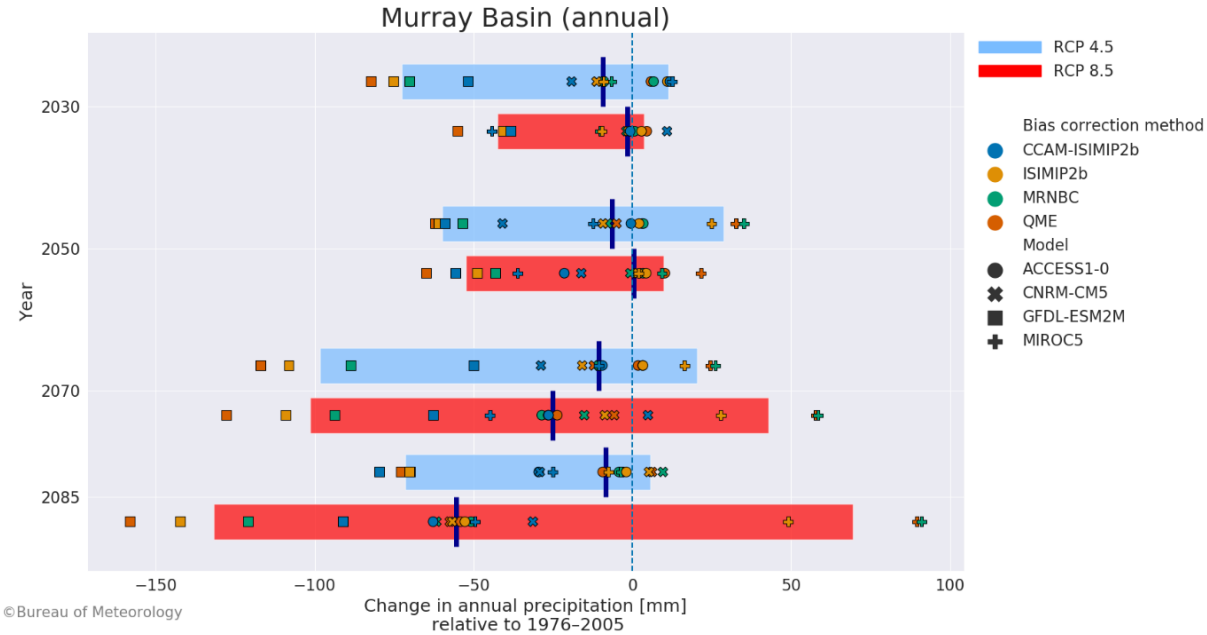

Figure 4.2. Change in annual precipitation (mm) projected by each ensemble member for 2030, 2050, 2070 and 2085 in the Murray Basin region. The red bar shows the 10th to 90th percentiles for RCP8.5. The blue bar shows the 10th to 90th percentiles for RCP4.5. The dark blue line shows the ensemble median. The change is relative to the reference period (1976–2005)

The spatial distribution of change in annual precipitation is shown in Figure 4.3 for the 4 time periods and the 2 representative concentration pathways. The largest decreases in annual precipitation are projected over the high-precipitation regions of the alps and Cape Otway. This is evident in both representative concentration pathways since both scenarios project decreases from mid-century. There is a tendency for dry conditions to increase from north to south of the Murray Basin region for both greenhouse gas emission scenarios. The projected decrease in median annual precipitation is greater under RCP8.5 than RCP4.5 in the latter part of the century (Figure 4.2).

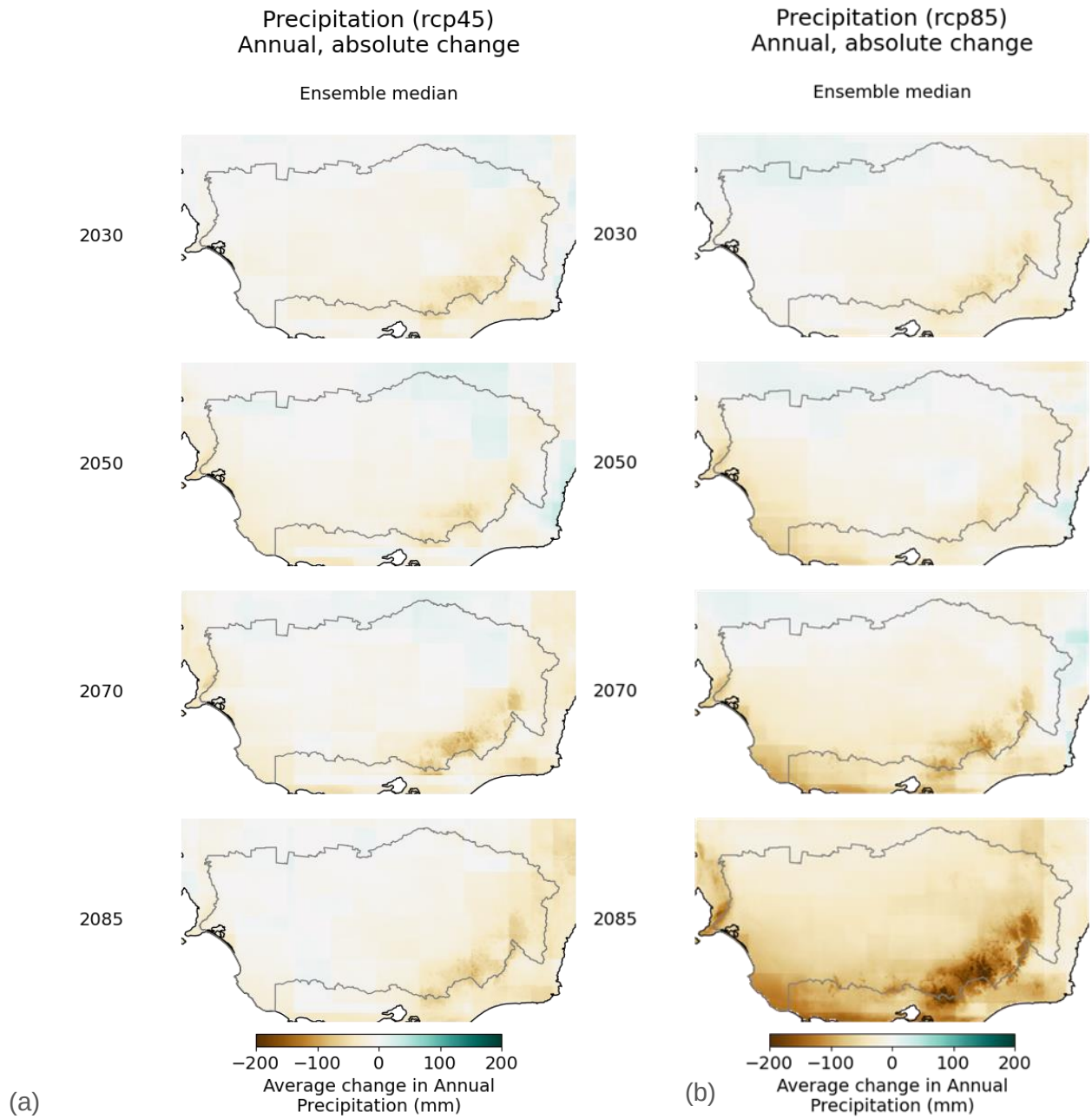

Figure 4.3. Absolute change (mm) (median) in annual modelled precipitation projected across the Murray Basin region for 2030, 2050, 2070 and 2085 under (a) RCP4.5 and (b) RCP8.5. The change is relative to the reference period (1976–2005)

Projected changes for seasonal precipitation (Figure 4.4), particularly in the winter (June–August) months (Figure 4.4b), feature a very large model spread and include both wetter and drier futures. The ensemble median projects a decrease under both representative concentration pathways by around 10% by mid-century, with further reductions possible towards the end of the century. Ensemble members downscaled by CCAM_ISIMIP2b tend to simulate drier future conditions under higher levels of greenhouse gases, possibly linked to a better representation of the changing weather interactions with the mountains (e.g. Grose et al. 2019). By the end of the century, projected changes under both representative concentration pathways are around −30.5 mm to +16.9 mm in winter and around −43.4 mm to +7.6 mm in spring.

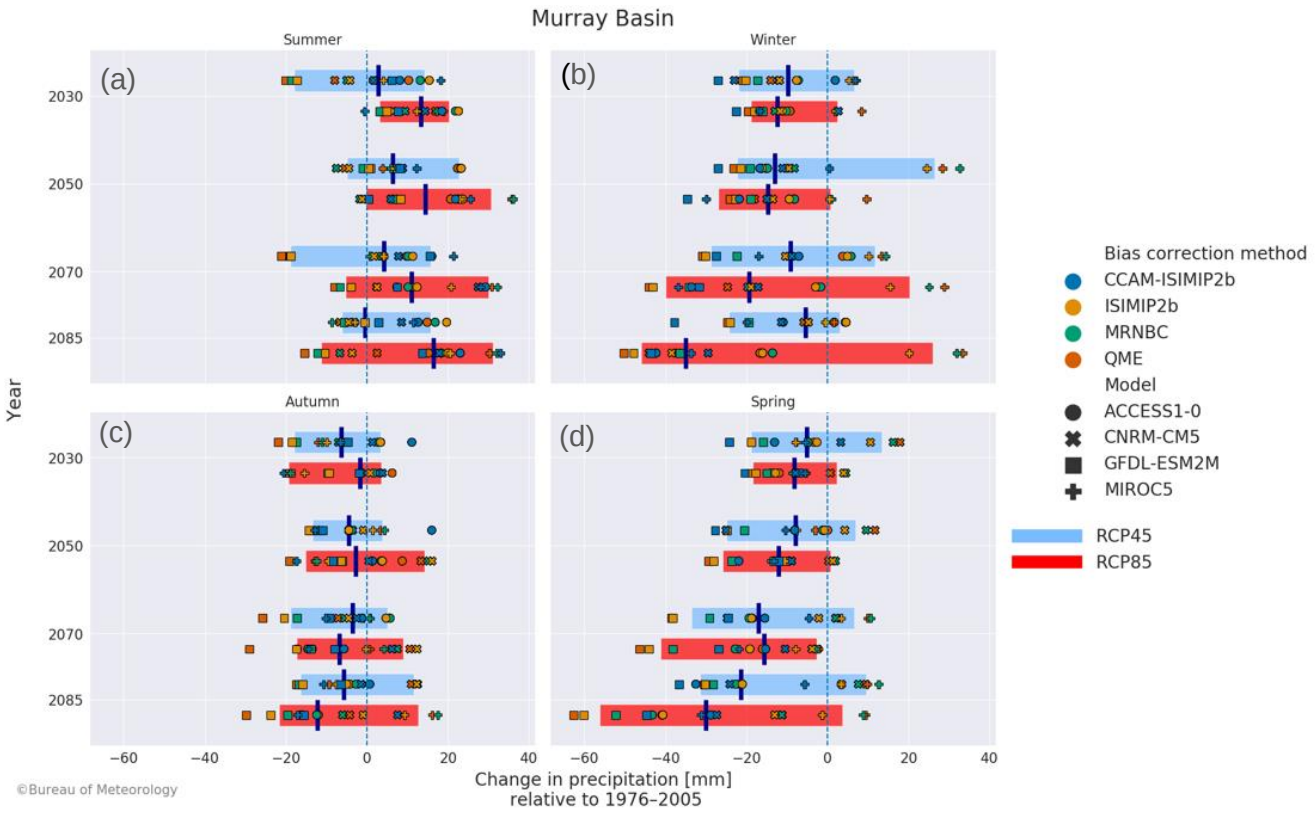

Figure 4.4. Absolute change in modelled precipitation (mm) projected by each ensemble member for (a) summer (December–February), (b) winter (June–August), (c) autumn (March–May) and (d) spring (September–November) for 2030, 2050, 2070 and 2085 in the Murray Basin region. The red bar shows the 10th to 90th percentiles for RCP8.5. The blue bar shows the 10th to 90th percentile for RCP4.5. The dark blue line shows the ensemble median. The change is relative to the reference period (1976–2005)

There is a large spread in projections of summer precipitation, but in some time periods, particularly under RCP8.5, an increase in precipitation is favoured (Figure 4.4a). A projected increase in summer precipitation would likely not be effective in contributing to runoff given higher evapotranspiration rates. The dynamically downscaled CCAM_ISIMIP2b ensemble members tend to project wetter summer precipitation, possibly due to the effect that CCAM captures convective processes associated with topography in mountainous regions (Grose et al. 2019). During the warm season, local land-atmosphere processes may become more important, as indicated by increases in localised thunderstorms over recent decades (Pepler et al. 2020). Precipitation increases are also projected to be associated with a southward expansion of the sub-tropical ridge (STR) (Figure 2.2) (Hope et al. 2017). Localised summer precipitation requires high-resolution climate models – even higher than the resolution provided by CCAM – increasing the uncertainty of summer precipitation projections.

Autumn precipitation projections feature a large spread in our 16-member ensemble with both large increases and large decreases plausible (Figure 4.4c), but the change signal is less strong than any other season. The little change projected by the ensemble median does not align with observed trends in recent decades. Additionally, the simulation of the current climate in autumn is known to have deficiencies (Hope et al. 2015). A ‘seasonal paradox’ between observations and CMIP5 model projections in the spring and autumn seasons is indicated, with strong and consistent drying projected for spring and less drying projected for autumn, the reverse of the observed trends over the last 50 years.

The assessment summary for precipitation is given in Table 4.1.

Table 4.1. Assessment summary for precipitation for the Murray Basin region

Feature	Largest plausible range of change	Additional evidence: plausible process	Additional evidence: ability to simulate	Summary statement
Cool-season precipitation (May–Oct)	RCP4.5 −79 to 34 mm/season (−28% to 12%) RCP8.5 −118 to 39 mm/season (−42% to 15%)	Precipitation decreases have been observed in recent cool seasons, mainly autumn and spring. Increasing pressure (e.g. STR) and reduced upper-level lows are expected to reduce the precipitation in the future, which aligns with a decrease in cool-season precipitation already observed for the region.	Higher resolution modelling will capture the weather interactions with the mountains better (e.g. CCAM_ISIMIP2b). The influence from CCAM_ISIMIP2b is a push towards a drier projection.	Increases and decreases are both plausible. Evidence such as the observed precipitation decreases, and our good understanding of process support the idea that drier future conditions are more plausible than wetter conditions.
Warm-season precipitation (Nov-–April)	RCP4.5 −43 to 24 mm/season (−19% to 13%) RCP8.5 −41 to 53 mm/season (−18% to 28%)	Our understanding of how warm-season weather will respond to a changing climate is low; however, summer precipitation extremes are likely to increase in intensity. More thunderstorm activity is suggested, and a southward shift of the STR means more of Murray Basin will be influenced by tropical precipitation.	Accurately projecting thunderstorms requires high spatial and temporal resolution not achieved in any projection data.	Changes to warm weather precipitation are uncertain due to poor process understanding and low model agreement. Very large increases and decreases are both plausible. Natural inter-annual variability will continue to be an important climate feature. Extremes are likely to increase in intensity (see 4.6.1).

4.3 Runoff

Mean annual runoff projections range from little change to large decreases, with most ensembles tending towards drier futures. Notably, there is no significant difference in projections between representative concentration pathways in terms of magnitude of ensemble spread (Figures 4.5 and 4.6). However, by late century (2070 time period and beyond) the ensemble median for RCP8.5 projects larger decreases than that of RCP4.5, following the precipitation trend. The natural high inter-annual variability of runoff is projected to remain a key feature of the region's hydrology to late century (ACCESS1-0_ISIMIP2b) (Figure 4.5).

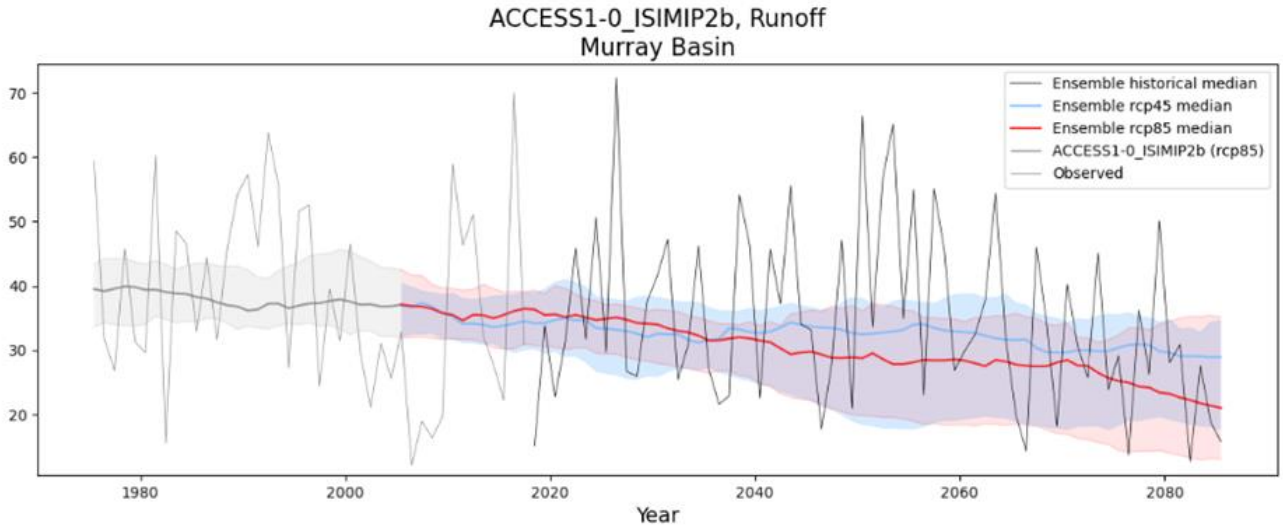

Figure 4.5. Annual modelled runoff (mm) projected to 2099 by ensemble members for RCP4.5 (blue) and RCP8.5 (red) greenhouse gas emission scenarios in the Murray Basin region. The shaded areas represent the 10th to 90th percentile range for all ensemble members in the historical and future time periods. The time series for ACCESS1-0_ISIMIP2b (RCP8.5) is included (dotted line) to show the variability projected for an individual ensemble member. The grey line represents the modelled historical median runoff

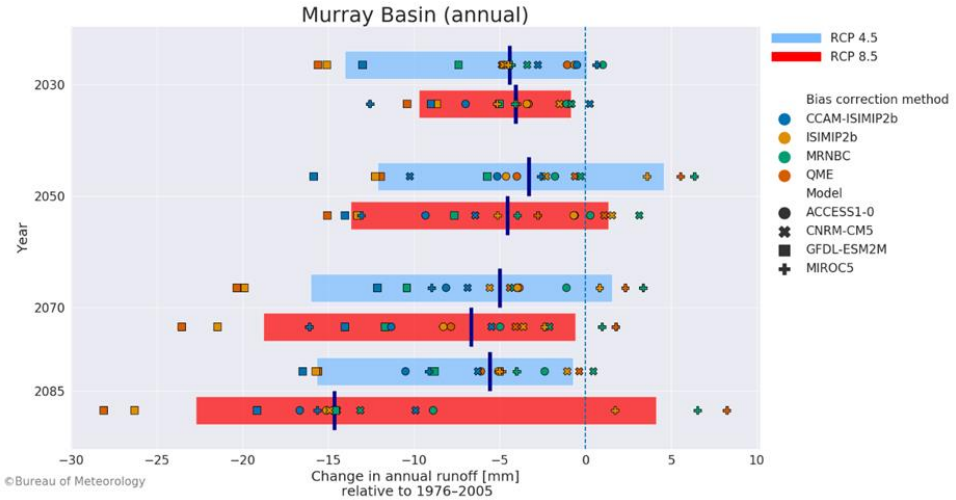

Figure 4.6. Absolute change in annual runoff (mm) projected by each ensemble member for 2030, 2050, 2070 and 2085 in the Murray Basin region. The red bar shows the 10th to 90th percentiles for RCP8.5. The blue bar shows the 10th to 90th percentile for RCP4.5. The dark blue line shows the ensemble median. The change is relative to the reference period (1976–2005)

There is a significant variation in projected spatial change in runoff in the Murray Basin region (Figure 4.7). The important catchments supplying large surface storage systems along the Great Dividing Range (in southern and south-eastern regions) feature much stronger signals for decreases in all seasons. This is related to the larger decreases in precipitation projected for these regions in particular during the winter and spring months. The alpine regions project the annual greatest decrease, with a larger decrease in RCP8.5 than RCP4.5. In the low-lying western part of the region, projections vary from little change to large increases in the warmer months. However, in this part of the region, runoff is small and would make projected changes highly sensitive to even small increases.

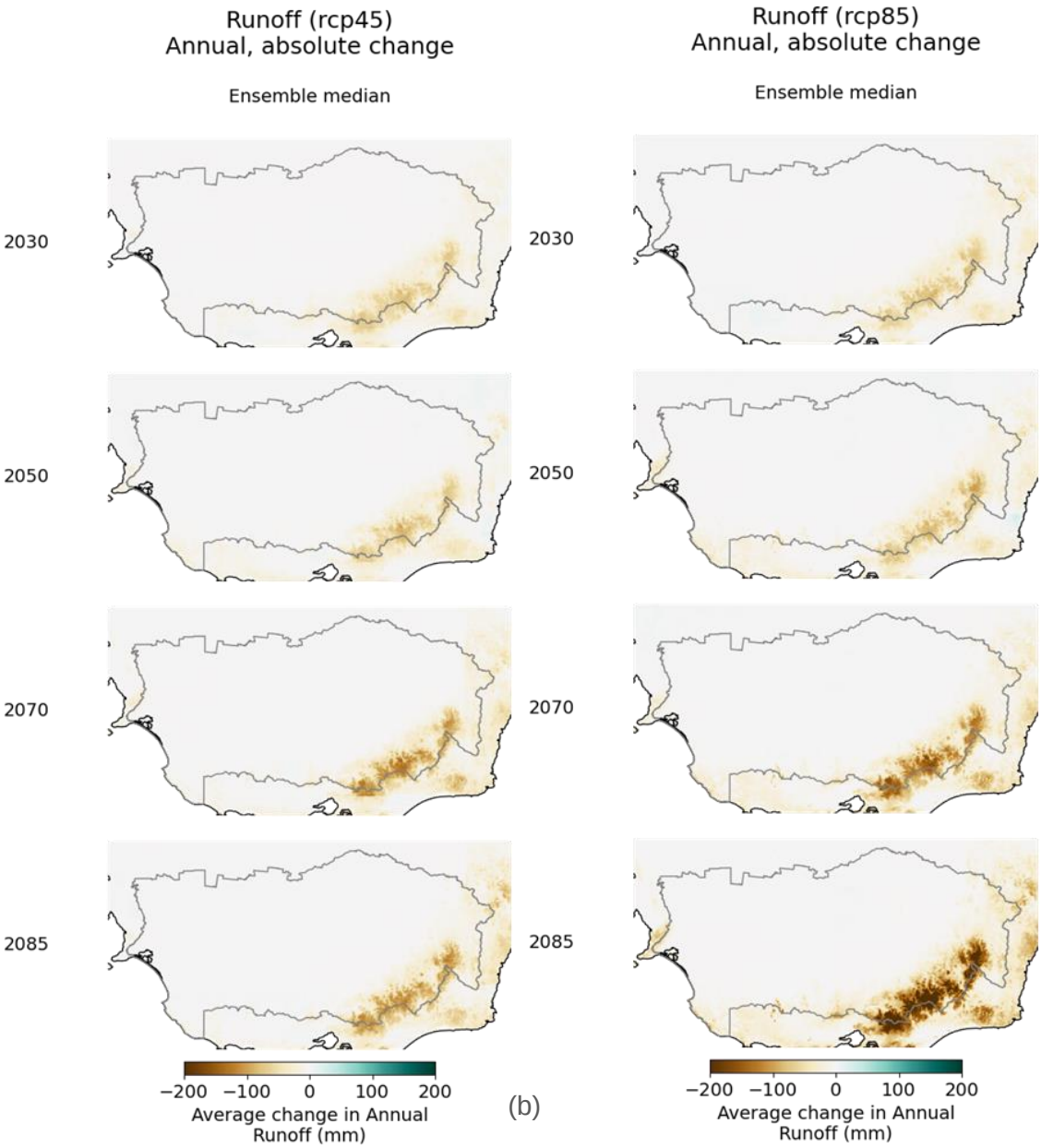

Figure 4.7. Absolute change (mm) (median) in annual runoff projected across the Murray Basin region for 2030, 2050, 2070 and 2085 for (a) RCP4.5 and (b) RCP8.5. The change is relative to the reference period (1976–2005)

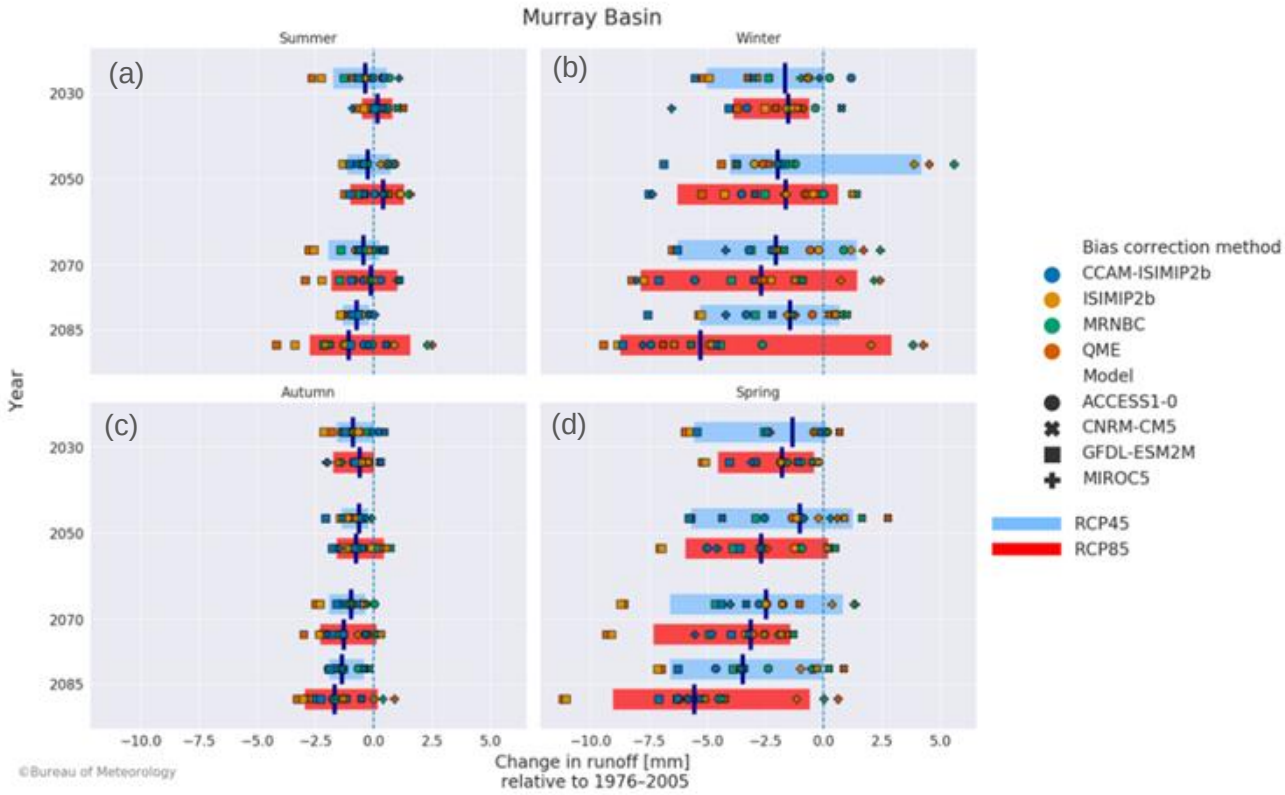

Figure 4.8. Absolute change (mm) in modelled runoff projected by each ensemble member for (a) summer (December–February), (b) winter (June–August), (c) autumn (March–May) and (d) spring (September–November) for 2030, 2050, 2070 and 2085 in the Murray Basin region. The red bar shows the 10th to 90th percentiles for RCP8.5. The blue bar shows the 10th to 90th percentile for RCP4.5. The dark blue line shows the ensemble median. This change is relative to the reference period (1976–2005)

While projections in ensemble median summer runoff are for little change or drier for both representative concentration pathways (Figure 4.8a), both increases and decreases are also plausible. It is interesting to note that the projected wetter precipitation conditions in summer do not translate into larger projected runoff. This is related to projected high potential evapotranspiration and drier soil moisture at the end of the spring season – increased precipitation on drier catchments may generate disproportionally low runoff.

Most storylines project decreases in runoff for autumn and spring (Figure 4.8c, d). The ensemble median projects a decrease by late century of about 28% under RCP4.5 and about 45% under RCP8.5. Most storylines project decreases in winter runoff, but increases are also projected (Figure 4.8b). These magnitudes follow the change signal of soil moisture in winter. The large spread in results reflects the large spatial variability in winter precipitation. However, for higher altitude areas in the south and south-east of the Murray Basin region, most of our storylines project large decreases.

The summary of confidence assessment for runoff is given in Table 4.2.

Table 4.2. Assessment summary for runoff in the Murray Basin region

Feature	Largest plausible range of change	Observed trends	Additional evidence: plausible process/ model reliability	Summary statement
Cool-season runoff	RCP4.5 −15 to 6 mm/season (−52% to 21%) RCP8.5 −20 to 4 mm/season (−71% to 19%)	Decreases in cool-season runoff observed in all 53 flow data sites for winter and spring, and 43 sites in autumn	100% of sites match the historical trend in reduced streamflow direction in winter. Evaluations show a large bias (between −5% and −20%) with a tendency to underestimate runoff.	Increases and decreases are projected for cool-season runoff. Decreases are projected in alpine regions, aligning with process understanding and observed trends.
Warm-season runoff	RCP4.5 −6 to 0.9 mm/season (−38% to 5%) RCP8.5 −8 to 4 mm/season (−53% to 32%)	Increases (16 sites) and decreases (35 sites) observed in flow data (and 2 sites show little change)	77% of sites match the trend direction in summer. Evaluations show large bias (between −5% and −20%) with a tendency to underestimate runoff.	Increases and decreases are projected for warm-season runoff, but changes are relative small in absolute terms.

4.4 Soil moisture

Large inter-annual variability, which is a feature of the current catchment conditions, is projected to remain a key feature under future conditions (shown by the example of ensemble member ACCESS1-0_ISIMIP2b in Figure 4.9).

Compared to current conditions, projected averages for annual root zone soil moisture range from little change to large decreases (Figure 4.10). There is a tendency towards decreasing soil moisture based on the majority of storylines results. Notably, the range of ensemble spread differs little between the representative concentration pathways. By late in the century (2070 period onward), the ensemble median under RCP8.5 projects decreases larger than projections for the median under RCP4.5.

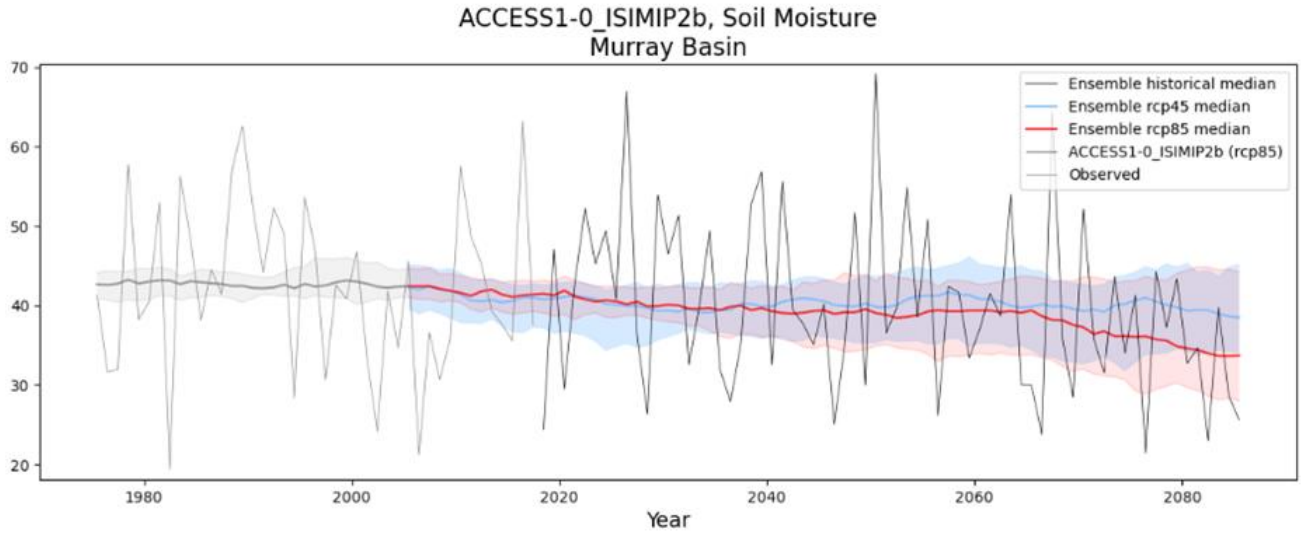

Figure 4.9. Annual modelled root zone soil moisture projected to 2099 by ensemble members for RCP4.5 (blue) and RCP8.5 (red) in the Murray Basin region. The shaded areas represent the 10th to 90th percentile range for all ensemble members in the historical and future time periods. The time series for ACCESS1-0_ISIMIP2b (RCP8.5) is included (dotted line) to show the variability projected for an individual ensemble member. The grey line represents the modelled historical median soil moisture

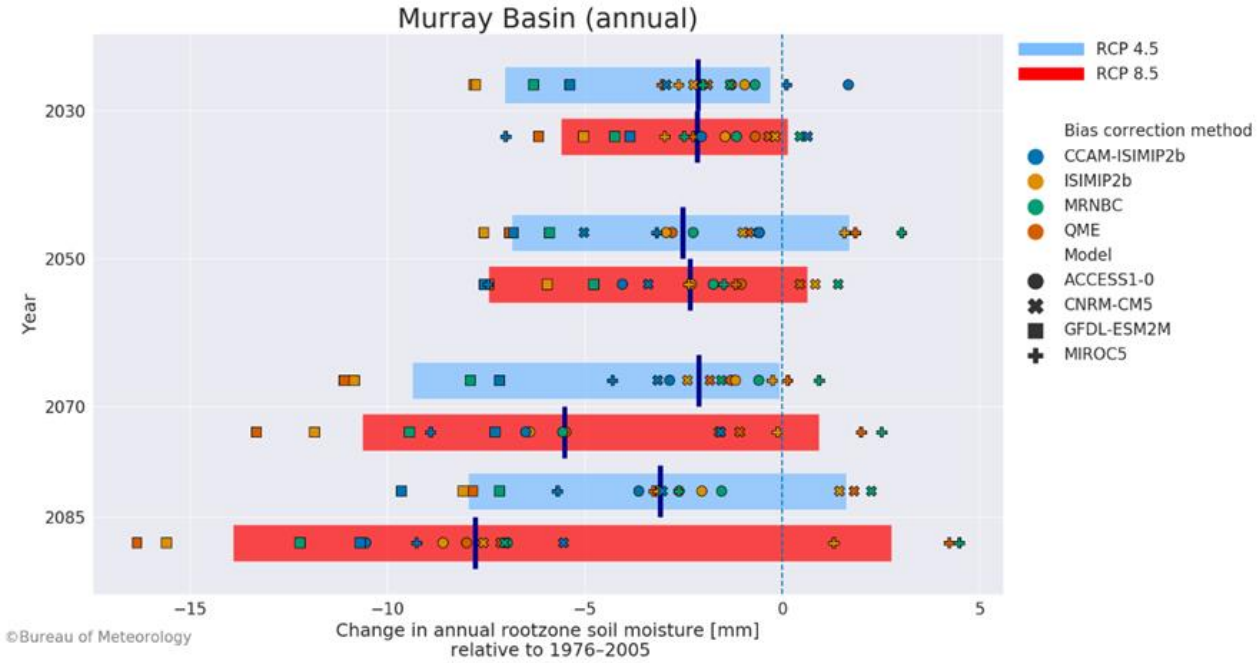

Figure 4.10. Absolute change (mm) in annual root zone soil moisture projected by each ensemble member for 2030, 2050, 2070 and 2085 in the Murray Basin region. The red bar shows the 10th to 90th percentiles for RCP8.5. The blue bar shows the 10th to 90th percentiles for RCP4.5. The dark blue line shows the ensemble median. The change is relative to the reference period (1976–2005)

The spatial distribution of the change in annual root zone moisture is shown in Figure 4.11. The largest projected decreases in soil moisture conditions occur in the alpine regions of the Murray Basin region. The western part of the Murray Basin region receives little precipitation and remains dry most of the time, and this is projected to continue as evidenced by the small change in soil moisture.

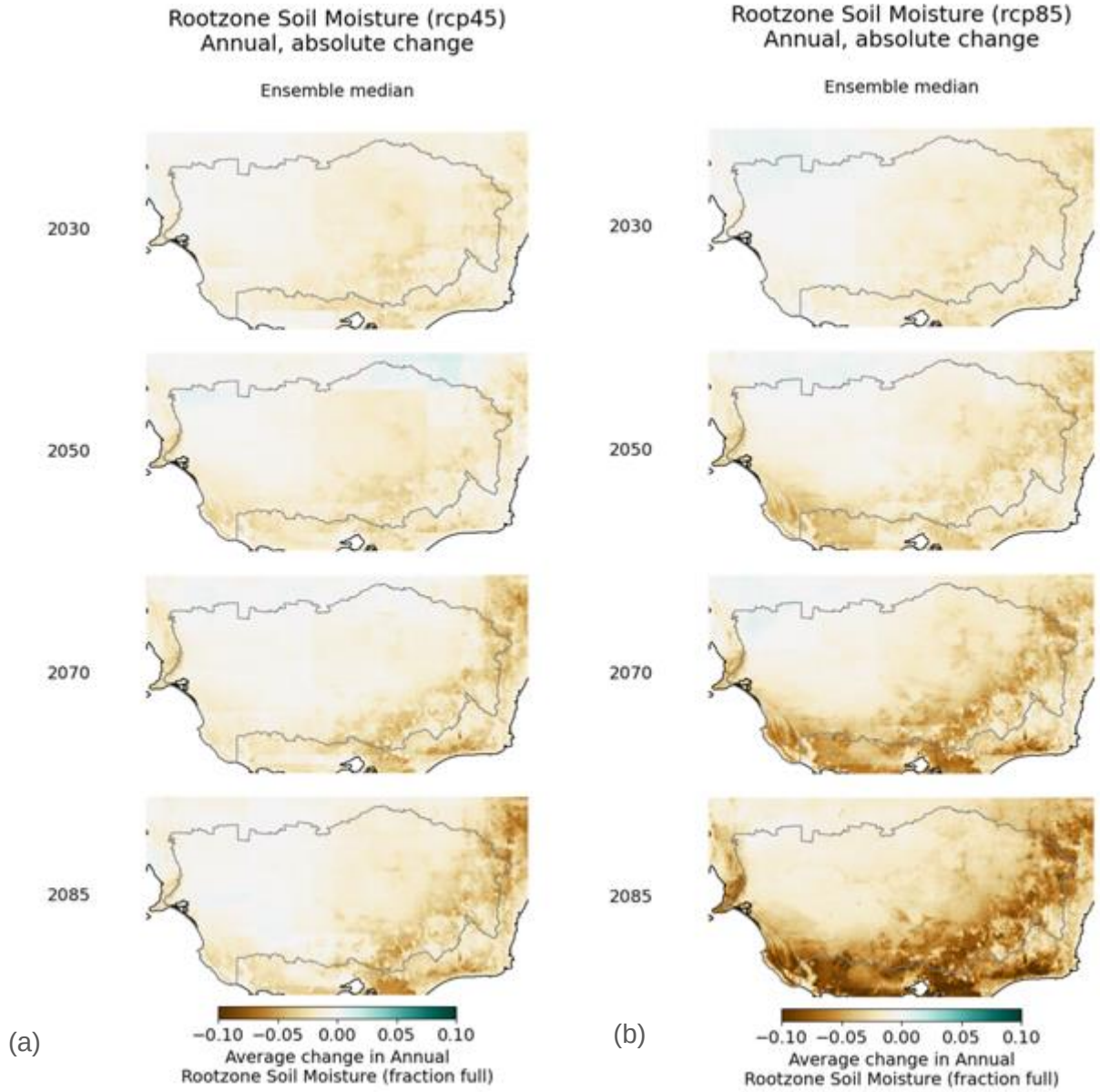

Figure 4.11. Absolute change (fraction full) (ensemble median) in annual root zone soil moisture projected for 2030, 2050, 2070 and 2085 for (a) RCP4.5 and (b) RCP8.5 across the Murray Basin region. The change is relative to the reference period (1976–2005). Fraction full (scale 0-1) is equivalent to % full/100 and represented the fraction of available water content in the root zone (0–1 m) soil profile

Soil moisture ensemble median projections indicate little change in the summer season, but the model spread is high, and both increases and decreases are plausible for both representative concentration pathways (Figure 4.12a). Drier soil moisture conditions are projected for the important autumn, winter and spring seasons with a high level of model agreement; enhanced drying is projected under RCP8.5 by the end of the century (Figure 4.12b–d). Some increases in soil moisture are projected for winter and autumn, but these increases are restricted to the low-lying inland regions. The higher altitude regions project decreases for all ensemble members.

Projected changes in soil moisture are strongly influenced by the projected changes in precipitation and tend to be more negative due to the projected increase in potential evapotranspiration related to increasing temperatures.

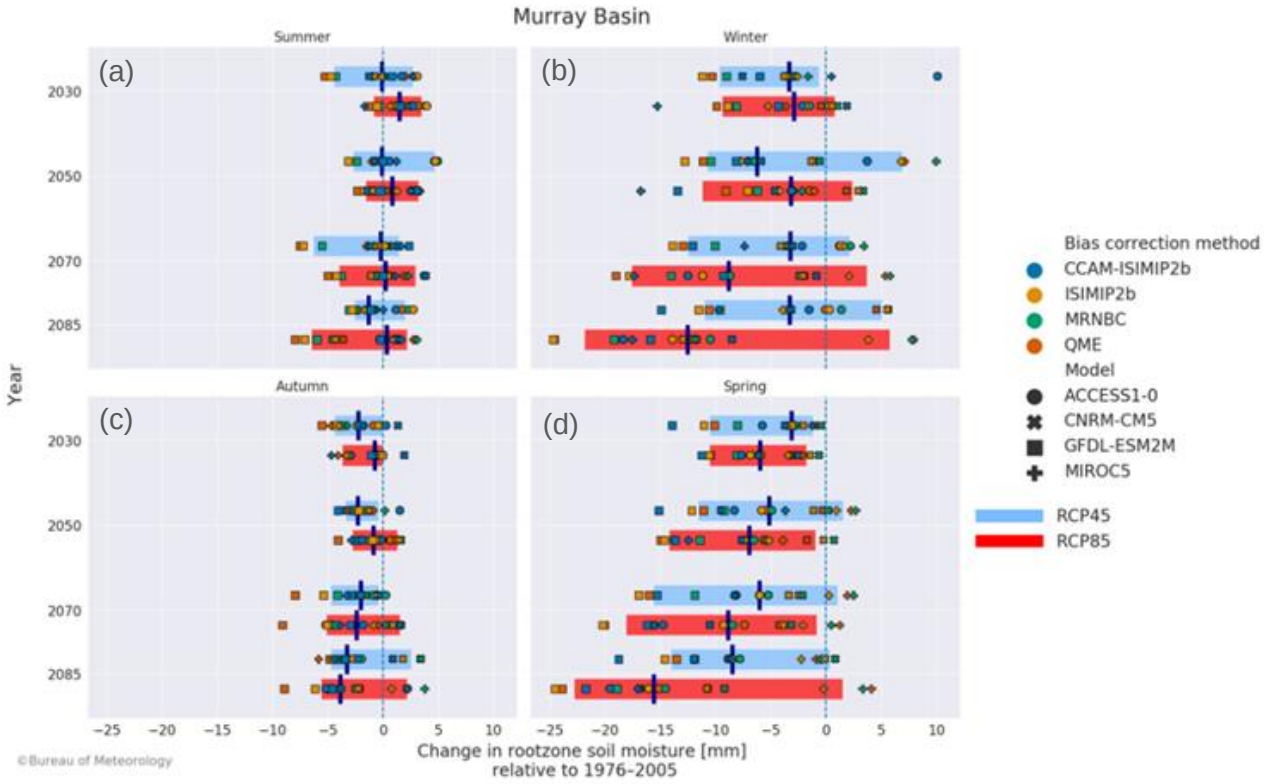

Figure 4.12. Absolute change (as fraction full of soil moisture capacity) projected by each ensemble member for (a) summer (December–February), (b) winter (June–August), (c) autumn (March–May) and (d) spring (September–November) soil moisture for 2030, 2050, 2070 and 2085 in the Murray Basin region. The red bar shows the 10th to 90th percentiles for RCP8.5. The blue bar shows the 10th to 90th percentile for RCP4.5. The dark blue line shows the ensemble median. The change is relative to the reference period (1976–2005)

The assessment summary for projected soil moisture in given in Table 4.3.

Table 4.3. Assessment summary for root zone soil moisture in the Murray Basin region

Feature	Largest range of change	Additional evidence: process understanding	Additional evidence: plausible process/ model reliability	Summary statement
Cool-season soil moisture (May–Oct)	RCP4.5 −6 to 2 mm/season (−30% to 11%) RCP8.5 −10 to 2 mm/season (-43% to 10%)	Changes to soil moisture are driven by seasonal average potential evapotranspiration and precipitation changes.	The overall bias low, generally 3% to 5% underestimation of soil moisture in all seasons. Very large positive and negative soil moisture bias from QME.	Increases and decreases plausible for cool-season soil moisture.
Warm-season soil moisture (Nov–April)	RCP4.5 −3 to 0.5 mm/season (−25% to 4%) RCP8.5 −4 to 2 mm/season (−26% to 13%)			Very large decreases in soil moisture are plausible under both greenhouse gas emission scenarios. RCP8.5 also projects increases, RCP4.5 largest projected increase is 4.5 mm.

4.5 Potential evapotranspiration

In the hydrological cycle, evapotranspiration plays an important role, particularly in soil evaporation and crop transpiration. While precipitation is the key driver of water availability, potential evapotranspiration is an indicator of potential losses in the total water balance for a system, and a limiting factor in the amount of water available for use. While these trends in potential evapotranspiration do not tell us what the projected changes to the actual evapotranspiration rate are, the signal indicates that the region could see impacts including:

- an increase in crop water demand (through higher transpiration of plants)
- increased evaporation from soils following a higher depletion rate of soil moisture
- the potential for greater losses from surface water storages through evaporation.

The annual potential evapotranspiration across the Murray Basin region is projected to increase in the future, consistent with an increase in temperatures (Figures 4.13 to 4.15). The time series of annual potential evapotranspiration for the region for the ACCESS1-0_ISIMIP2b ensemble member is shown in Figure 4.13. This clearly projects an increase in annual potential evapotranspiration in the future, with increases proportionate to emissions scenarios and thus very large increases projected by both scenarios by late century. Increases are projected in all seasons, with the largest projected increases in seasonal potential evapotranspiration expected during spring (Figure 4.15d). It is, however, not clear what could cause the projected largest increase in potential evapotranspiration in the spring period.

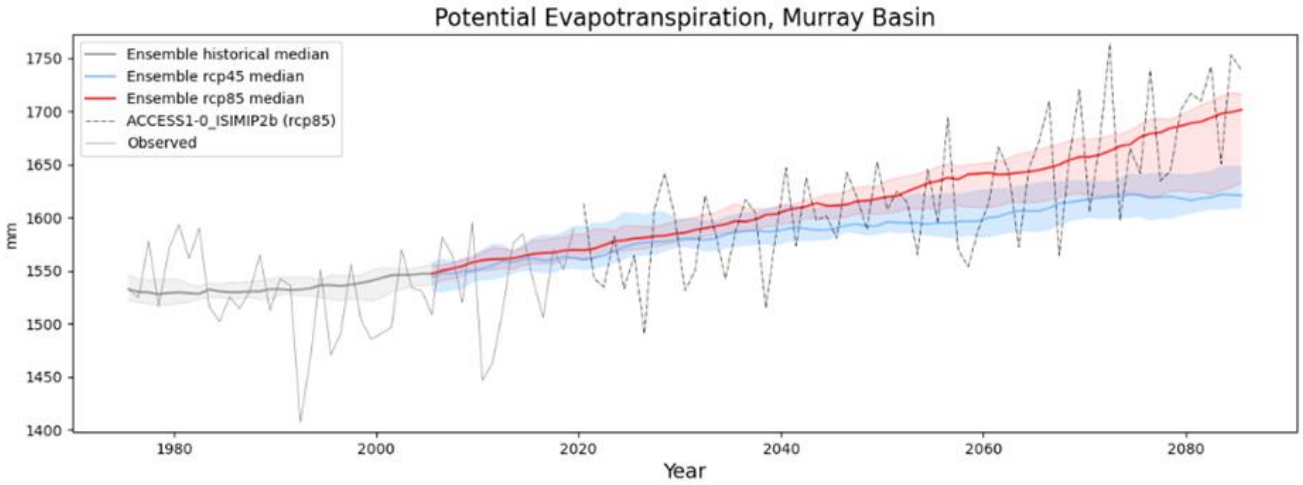

Figure 4.13. Annual modelled potential evapotranspiration (mm) projected to 2099 by ensemble members for RCP4.5 (blue) and RCP8.5 (red) in the Murray Basin region. The shaded areas represent the 10th to 90th percentile range for all ensemble members in the historical and future time periods. The time series for ACCESS1-0_ISIMIP2b (RCP8.5) is included (dotted line) to show the variability projected for an individual ensemble member. The grey line represents the modelled historical median potential evapotranspiration

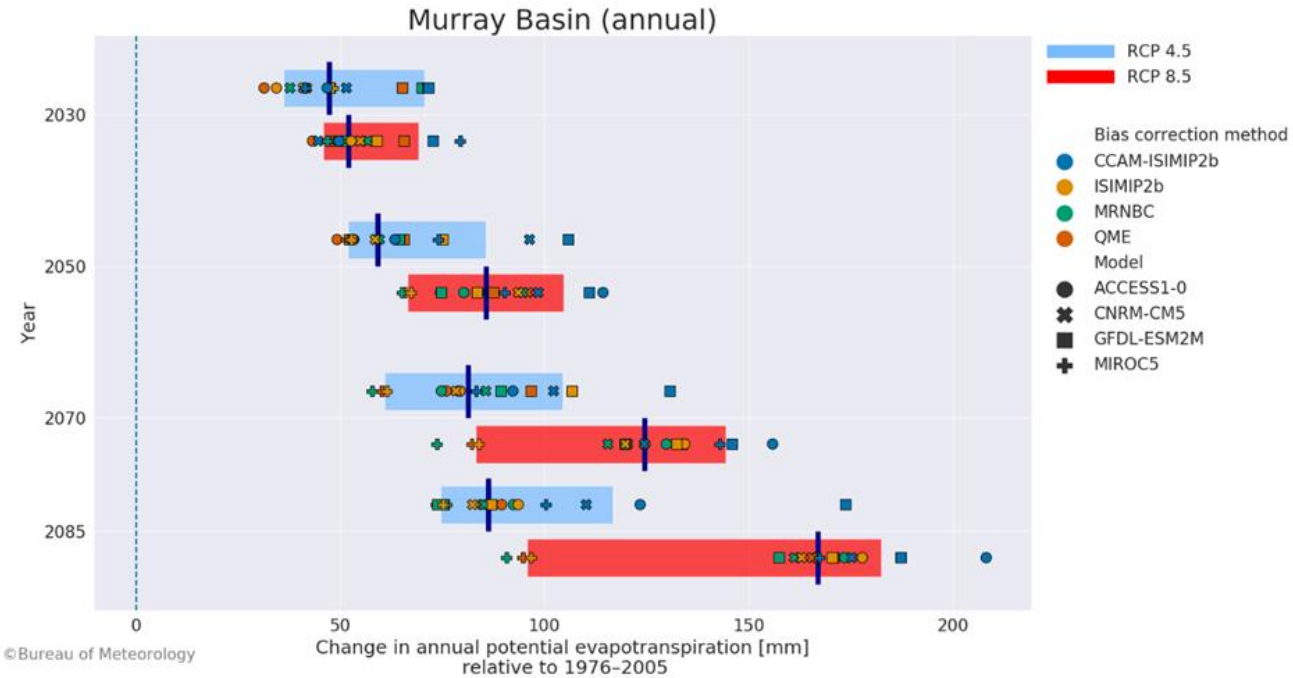

Figure 4.14. Absolute change (mm) in annual potential evapotranspiration projected by each ensemble member for 2030, 2050, 2070 and 2085 in the Murray Basin region. The red bar shows the 10th to 90th percentiles for RCP8.5. The blue bar shows the 10th to 90th percentiles for RCP4.5. The dark blue line shows the ensemble median. The change is relative to the reference period (1976–2005)

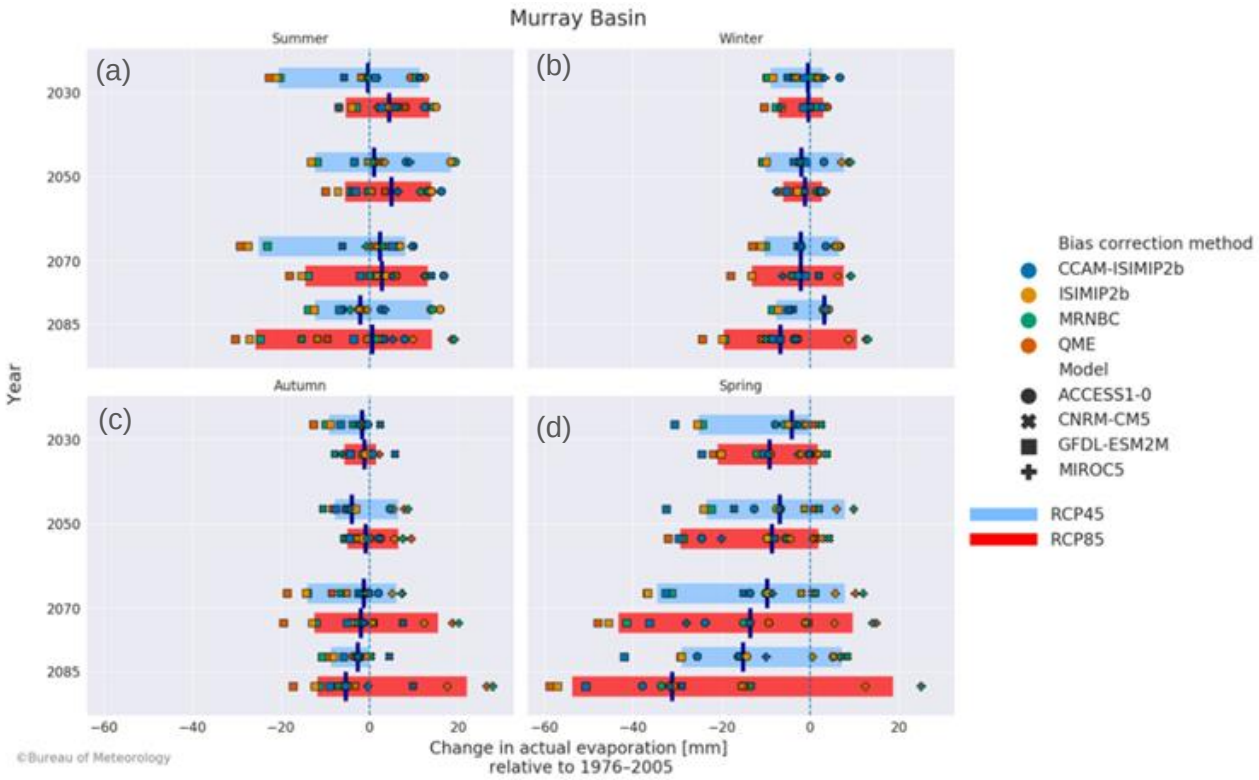

Figure 4.15. Absolute change (mm) in potential evapotranspiration projected by each ensemble member for (a) summer (December–February), (b) winter (June–August), (c) autumn (March–May) and (d) spring (September–November) for 2030, 2050, 2070 and 2085 in the Murray Basin region. The red bar shows the 10th to 90th percentiles for RCP8.5. The blue bar shows the 10th to 90th percentile for RCP4.5. The dark blue line shows the ensemble median. The change is relative to the reference period (1976–2005)

The assessment summary for the projected potential evapotranspiration is given in Table 4.4.

Table 4.4. Assessment summary for potential evapotranspiration in the Murray Basin region

Feature	Largest plausible range of change	Additional evidence: process understanding	Additional evidence: plausible process/ model reliability	Summary statement
Annual potential evapotranspiration	RCP4.5 31 to 173 mm/year (2% to 11%) RCP8.5 43 to 208 mm/year (3% to 14%)	Small increase in evapotranspiration observed in the recent past. Aligned with process understanding that a warmer climate results in higher potential evapotranspiration.	Low bias in potential evapotranspiration simulation.	Increase in annual and seasonal potential evapotranspiration for both representative concentration pathways and in all seasons. Magnitude is proportionate to greenhouse gas emission concentration.

4.6 Extreme events

Hydrological extremes, including floods and droughts, are among the costliest natural disasters in the world (Wasko & Nathan 2019). They pose risks to life, food security, infrastructure and energy supply. Future climate change is expected to bring a more variable precipitation pattern with longer dry spells and more frequent extreme events, such as flood-producing rain and cyclones (Easterling et al. 2000; Johnson & Murray 2004; Milly et al. 2002; Palmer & Räisänen 2002; Walsh & Ryan 2000). On the extreme dry end of the spectrum, prolonged absence of precipitation, for example, through a failure of the monsoon, may result in increasing dry spells. On the extreme wet end of the spectrum, an increase in extreme rains can exacerbate flooding events. Changes in the frequency, amount and duration of precipitation have serious impacts on sectors such as agriculture, water management and flood control (Alam et al. 2018). The ability to project future climate can help improve irrigation planning, flood planning, and design and management of hydraulic structures such as dams and stormwater drainage systems. This knowledge will also help us identify Australia's vulnerability to future droughts and improve resilience through mitigation actions.

4.6.1 Extreme precipitation and runoff

Earlier studies using observations and projections have shown an increase in the frequency of extreme precipitation events in the Australian region (Alexander & Arblaster 2009; Rafter & Abbs 2009). In a warming climate, heavy precipitation events are likely to increase in magnitude due to the increased moisture-holding capacity of a warmer atmosphere (Sherwood et al. 2010; Yin et al. 2020). Such excessive precipitation events may enhance the potential risk of flooding, depending on antecedent conditions. However, Wasko & Nathan (2019) found that, in Australia as in many other parts of the world, soil moisture deficits that are first re-filled during precipitation events commonly reduce flood magnitudes, despite increasing precipitation extremes. Therefore, in this project, we estimated projected future flood scenarios based on both precipitation and runoff.

Characterising changes in flood frequency and intensity at a large spatial and temporal scale is challenging; flood risk often depends on local topography, sub-daily precipitation intensity and antecedent conditions. We calculated a set of threshold-based indicators using precipitation and runoff to capture changes in flood risk on a broad scale. The changes on the extreme wet end of the spectrum are determined using 3 indicators: the projected annual mean and maximum daily precipitation and runoff, and the 20-year return period precipitation and runoff estimated using the generalised extreme value (GEV) distribution. The GEV distribution is generally used to represent the rare events (Bali 2003), which are indicative of floods.

Both precipitation (Figure 4.16) and runoff (Figure 4.17) analyses show an increase in the maximum 1-day and 20-year return period for two 30-year periods (2030 and 2070) and both greenhouse gas emission scenarios (RCP4.5 and RCP8.5); the change in the 20-year return period for runoff is not as large as the change in maximum runoff. In comparison, the trends in the annual mean precipitation (Figure 4.16) clearly project that the ensemble median for mean precipitation tends towards little change or decrease. The ensemble median for runoff tends towards decrease (Figure 4.17). This pattern (little change or decrease in annual mean relative to increase in extremes) is found in almost all other National Hydrological Projections regions and is supported by the results from other studies (Abbs & Rafter 2009; Alexander & Arblaster 2009; Rafter & Abbs 2009; Wasko & Sharma 2017) and reflects a shift towards larger proportions of precipitation occurring in the form of high intensity events. The magnitudes of the simulated changes in extreme precipitation indicators depend heavily on the representative concentration pathways, the given ensemble member and the time period in question. Therefore, the magnitude of change is uncertain. This could be because smaller-scale systems that generate extreme precipitation are not well represented by GCMs (Fowler & Ekström 2009). Our analysis shows that the far future (2070 period, i.e. 2056–2085) has a wider spread in ensemble members than the near future (2030 period, 2016–2045). This is evident for both of precipitation and runoff-based estimated change in extreme wet conditions ((Figures 4.16 and 4.17), where the spread in the runoff indicators is higher than the spread in the precipitation indicators.

In summary, the results suggest that the intensity of extreme events is going to increase in the Murray Basin region. However, the magnitude and timing of the future change in intensity of wet extremes from natural climate variability of the region, cannot be projected with certainty.

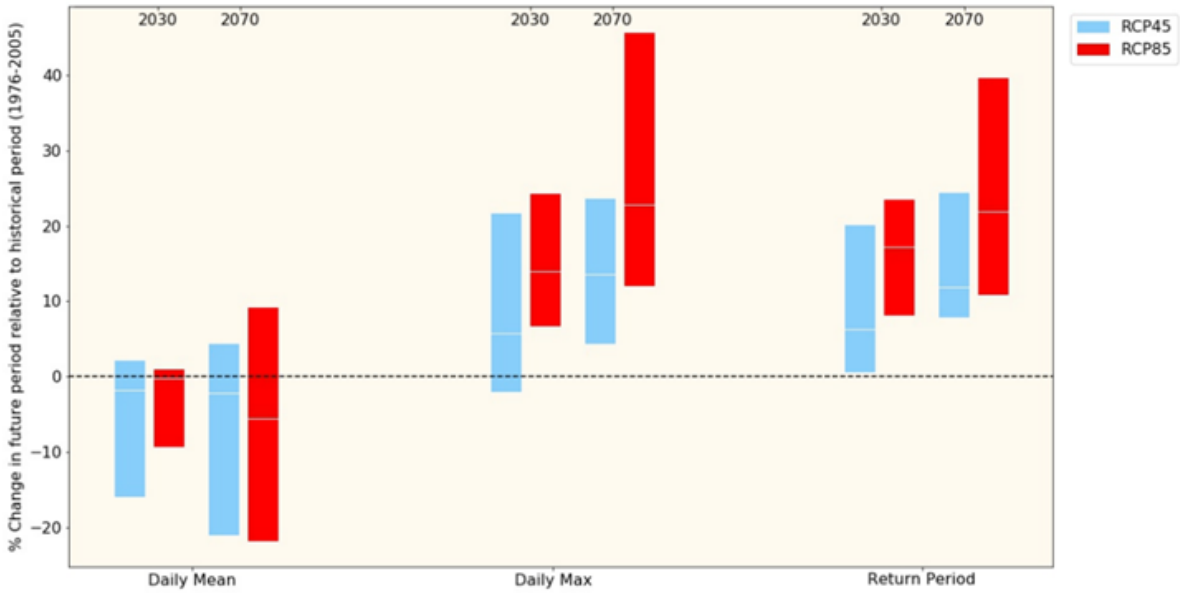

Figure 4.16. Future extreme wet analysis based on modelled precipitation shown by changes (%) in mean daily precipitation, maximum daily precipitation and 20-year return period of the annual maximum precipitation for 2030 and 2070 in the Murray Basin region. The red bars show the 10th to 90th percentiles for RCP8.5. The blue bars show the 10th to 90th percentiles for RCP4.5. The white lines show the ensemble median. The change is relative to the reference period (1976–2005)

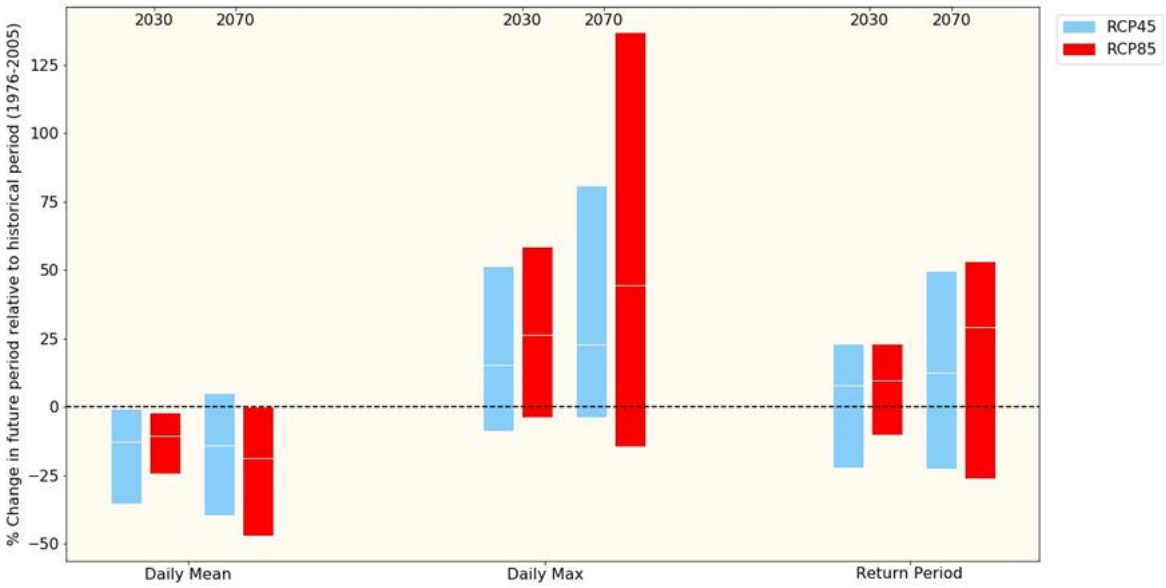

Figure 4.17. Future extreme wet analysis based on modelled runoff shown by changes (%) in mean daily runoff, maximum daily runoff and 20-year return period of the annual maximum runoff for 2030 and 2070 in the Murray Basin region. The red bars show the 10th to 90th percentiles for RCP8.5. The blue bars show the 10th to 90th percentiles for RCP4.5. The white lines show the ensemble median. The change is relative to the reference period (1976–2005)

4.6.2 Extreme dry landscape conditions

To gain a greater understanding of future extreme dry conditions or droughts and the range of socioeconomic impacts, it is important to combine multiple lines of evidence encompassing climatological and hydrological extreme dry states. Projected extreme meteorological, hydrological and agricultural dry conditions were investigated using 3 separate indicators. A meteorological extreme dry state refers to when an area is subject to below-average precipitation that results in dry landscape conditions. A hydrological extreme dry state refers to when water resources are insufficient, for example, in rivers and water storages. An agricultural extreme dry state is determined through the impacts of soil moisture deficits on crops and vegetation and its subsequent effect on livestock. Analysis of future conditions must also take into account different time frames, as hydrological dry states arise over a longer time period than meteorological and agricultural extreme dry periods (which can include 'flash droughts'). Hydrological dry states result from prolonged spells of below-average precipitation and the subsequent below-average runoff. However, a reduction in precipitation may result in a decrease in water available for stock or a depletion of topsoil moisture needed to grow crops. This will impact agriculturalists sooner than it will cause disruption to the whole hydrological system.

In this study, projected precipitation, runoff and soil moisture data was used to represent these 3 types of droughts: meteorological, hydrological and agricultural. This lets us capture the potential impacts on key sectors of agricultural and water-sensitive industries. The indicators are used as a proxy for drought, noting that they should be taken as an indicative estimate of drought conditions because many other factors involved in determining whether a region is in drought have not been included in this analysis.

As the various types of extreme dry conditions or droughts arise over different time frames, our analysis addresses short-term to long-term durations by calculating the median extreme dry condition duration (short, moderate, long or prolonged). An extreme dry condition is defined by applying a threshold quantile of 15% of the historical period to future projections. We use percentile thresholds to determine drought periods as this method involves no assumptions about the data distribution. Using the 15th percentile as the drought threshold means that any month below this threshold is classified as being in drought. The 15th percentile corresponds approximately to a threshold of −1 for the widely used Standardised Precipitation Index (SPI) (McKee et al. 1993) and is commonly used to characterise 'moderate' droughts (McKee et al. 1993). We use this threshold to ensure we have a sufficient number of drought events to infer trends in drought metrics reliably. Previous work has shown that while simulated drought characteristics can be somewhat sensitive to the choice of threshold, inter-model differences represent a much greater source of uncertainty (Ukkola et al. 2018). The 15% threshold definition is applied separately for each indicator and for each different time period. Figure 4.18 and Table 4.5 show that various characteristics of the extreme dry condition were evaluated, namely, the future change in the cumulative duration of the short, moderate, long and prolonged extreme dry spells and the change in the spatial extent of the area undergoing short, moderate, long, and prolonged extreme dry conditions compared to the historical reference period (1976–2005). Using the defined drought metrics, the average percentage of time spent in drought in the future was also calculated and is presented below in Table 4.5.

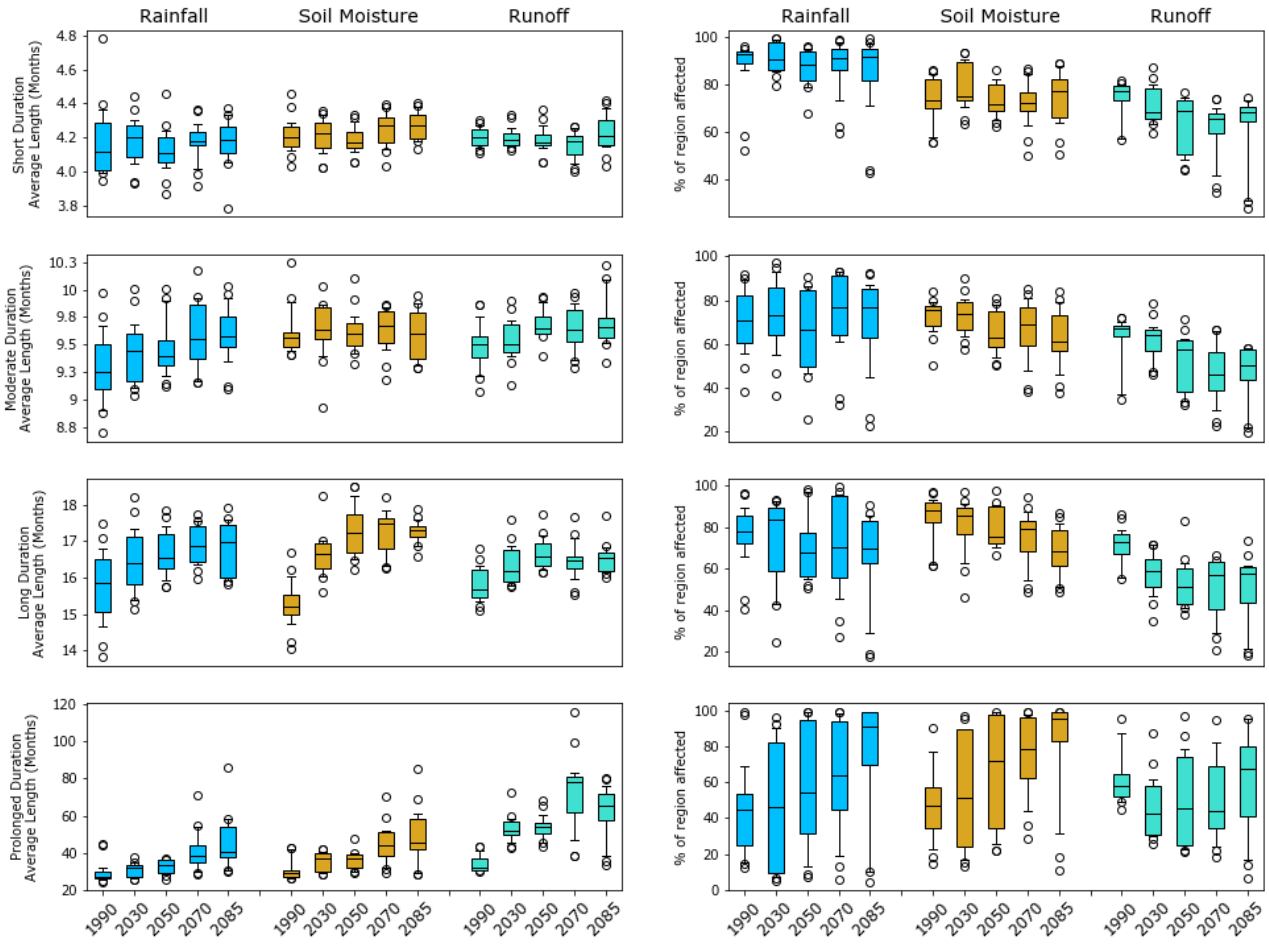

Figure 4.18. Change in projected median drought lengths (left) and percentage of total area affected by extreme dry conditions (right) for modelled precipitation (meteorological drought indicator), modelled soil moisture (agricultural drought indicator) and modelled runoff (hydrological drought indicator) in the Murray Basin region. The box plots show the median, 10th and 90th percentiles and outliers. They are presented for short-term, moderate, long-term and prolonged drought durations. The change is relative to the reference period (1976–2005)

Table 4.5 Summary of the primary results shown in Figure 4.18

Duration (months)	Drought type	Projected result	Impact
Short (3–6 months)	All types	Little change on average projected for all drought types in terms of duration but up to a 10% decrease in spatial extent of drought, where a wider ensemble spread is shown in the change in spatial extent.	Projected flash droughts, remain similar on average compared to the historical reference period. Higher variability is plausible for the drought-affected regions, tending towards a decrease in area affected.
Moderate (7–11 months)	All types	Little change on average projected for all drought types but up to a ~10% decrease in spatial extent of drought, where a wider ensemble spread is shown in the change in spatial extent.	Projected moderate droughts remain similar to the historical reference period with higher variability plausible for the drought-affected regions, tending towards a decrease in area affected.

Long term (12–23 months)	All types	Increases projected to varying degrees across the future time periods, where the maximum increase is seen in agricultural long-term drought conditions (>20%). Areas under drought are projected to decrease by as much as 30%, varying over the future time periods for all droughts.	Projected long-term droughts to increase, which could have negative implications for river health, water-dependent industries and agricultural systems in the future.
Prolonged (>24 months)	Meteorological dry conditions	Projected ~10-30% increase in time in drought across the future time periods. Projected increase in area under meteorological drought across the future time periods overall, ranging from –15% to 25%.	Projected increases in prolonged periods of low precipitation are plausible with an intensification of precipitation-deficient areas in the future.
	Hydrological dry conditions	Projected ~30-40% increase in time in drought varying across the future time periods. Projected decrease in area under hydrological drought across the future time periods, ranging from –20% to 0% at the end of the century.	Projected increase in prolonged periods of low-runoff states, which can lead to water supply shortages and insufficient environmental flows in the future (see Chapter 5).
	Agricultural dry conditions	Projected increase of between 10% to 35% in time in drought across the future time periods. Projected increase in area under agricultural drought across the future time periods overall, ranging from 7% to 40%.	Projected increase in prolonged soil moisture deficits and states are plausible, with an increase in drought-affected areas towards the end of the century. This can lead to impacts on crop and pasture growth as well as natural vegetation growth in the future.

In summary we are likely to see an increase in multi-year extreme dry conditions in the Murray Basin region; however, the spatial extent of future extreme dry condition is uncertain due to the spread of results across the ensemble. The socioeconomic implications of these results mean that water-sensitive industries, agriculture and water management in this region need to prepare for drier conditions and an unreliable year-to-year water supply, brought about by an increase in long-term to prolonged dry spells. Particularly, the increase in agricultural prolonged drought-affected areas means that this drier landscape could have implications for bushfire fuel, worsening bushfires in the future. The environmental implications for ecosystems and river health could be significant as these results project reduced availability of water for plants and less surface water, meaning more variable environmental flows.

5 Exploring future water resource impacts: applying selected storylines to the Murray Basin region

Projection results feature many sources of uncertainty, including uncertainty over future trajectories of atmospheric greenhouse gas concentrations, how a warmer climate will lead to changes in hydroclimatic features and feedback loops, and how well climate models will represent those features. Acknowledging these uncertainties, the National Hydrological Projections 16-member ensemble provides a unique opportunity to examine the impacts of plausible future changes on Australia's hydroclimate and its water resources. Projections provide a collection of possible future storylines rather than a forecast or likelihood of a specific outcome.

While the National Hydrological Projections 16-member ensemble does not represent every possible future outcome (e.g. of the CMIP5 climate models) for every possible future emissions profile, the ensemble members do represent a selection of internally consistent plausible hydroclimatic futures, or storylines, that let us investigate hydrological responses and inform adaptation planning. Storylines can be used to tie the projections results to a specific impact (Shepherd et al. 2018). We have selected single ensemble members that represent changes to hydrological features that define a selection of storylines for the Murray Basin region.

5.1 Exploring water-sensitive impacts

These storylines explore examples of projected changes to water security for the Riverina Murray. The relationship between source water and water use is highly complex in the Murray Basin region due to a high degree of regulation and a highly engineered water grid that can facilitate inter-valley transfers. In the context of the highly complex management structure, the conceptualised water supply and demand system used in these storylines is highly simplified. Nevertheless, this simplified representation of water availability and use is useful for a general understanding, as we are more concerned with identifying changes to processes and broad trends than quantifying impacts.

Changes to water supply and demand storylines are explored below. These storylines explore examples of projected changes to water security for the Riverina Murray. Cool-season (May–October) runoff into the Upper Murray River catchment is used as an indicator to represent changes to water supply. Warm-season soil moisture (November–April) in the downstream Riverina Murray is used as a proxy for changes to irrigation demand.

5.2 Establishing representative storylines

To determine plausible storylines reflecting range of changes to water availability, changes to cool-season runoff for each ensemble member are plotted against changes to warm-season soil moisture in Figure 5.1. This plot shows a number of storylines that can be used to represent the ranges of conditions from the perspective of changes in water supply and drivers of demand (Table 5.1).

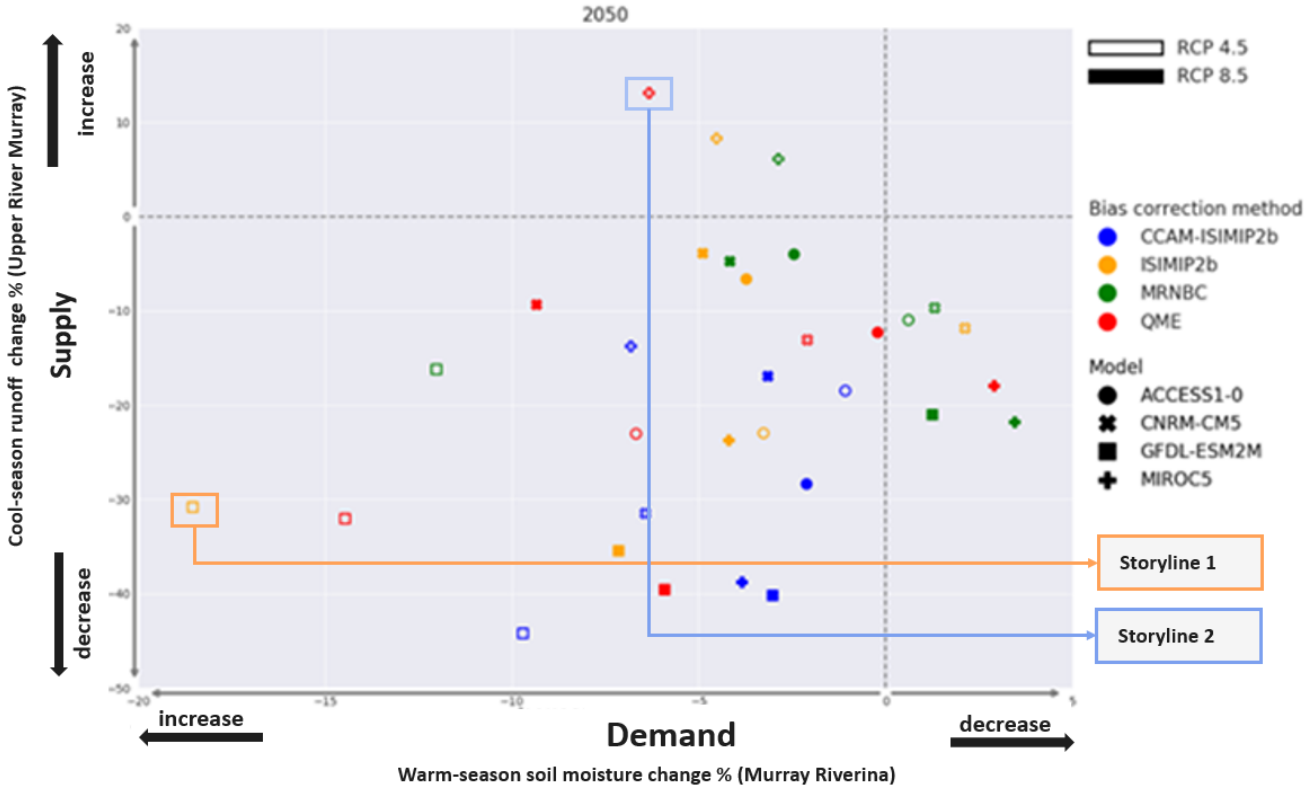

Figure 5.1. Projected changes to cool-season runoff vs projected changes to warm-season soil moisture. Wet season runoff is used as a proxy for changes to water supply and dry season soil moisture for changes to demand

Table 5.1. Storylines for exploring changes in water supply and drivers of demand

Storyline	Impacts to be explored
Large decreases in cool-season runoff, decreases in warm-season soil moisture (GFDL-ESM2M_ISIMIP2b RCP4.5)	Cool-season runoff is key for filling storages: what happens if seasonal runoff averages go down (37%) and irrigation area soil moisture goes down (7%) (i.e. demand increases)?
Increases in cool-season runoff (12%), decreases in warm-season soil moisture (7%) (MIROC5_QME RCP8.5)	Does an increase in cool-season runoff result in increased water availability when considering increases in demand in the warm season?

5.2.1 Storyline 1 – Large decreases in cool-season runoff, decreases in warm-season soil moisture (GFDL-ESM2M_ISIMIP2b RCP4.5)

This storyline is represented by the GFDL-ESM2M_ISIMIP2b climate model in RCP4.5 downscaled by the ISIMIP2b bias-correction and downscaling method. It represents the largest decreases in cool-season average runoff in 2050 (32% or 60 mm) compared to historic averages. Consequently, it projects the largest decreases in water supplies (based on seasonal totals). This storyline features a decrease in warm-season soil moisture of 17%, which is the largest projected decrease in soil moisture of any ensemble member in the warm months in 2050.

The large cool-season runoff decreases are driven by a combination of large decreases in cool-season precipitation and decreases in cool-season soil moisture associated with increased potential evapotranspiration and associated drying of catchments. The large warm-season decreases in soil moisture are associated with a 5% decrease in precipitation for this ensemble member, but also a 4% increase in potential evapotranspiration.

This storyline projects that impacts associated with reduced water availability will become more common over time. This pattern could potentially see lower allocations in average years, impacting on the price of water, which could rise, and reducing the security of water entitlements. While wet years and dry years are still projected to continue into the future, this storyline projects that the system could be less resilient to periods of drought as, on average, less water could be stored prior to periods of extended dry. Cool-season precipitation and runoff are typically reliable in this region (i.e. there is relatively low year-to-year variability), but the region has also seen extended dry periods with less reliable water availability (e.g. during the Millennium drought from 1996 to mid-2010).

The natural reliability of water availability could decrease under this storyline, increasing the degree of variability and resulting in more frequent and more extreme periods of extreme dry. Additionally, the increased demand in the irrigation districts (indicated by decreasing warm-season soil moisture) would compound the water security impacts associated with decreases in runoff in the storage catchments, and groundwater would also be affected. In this storyline, rain-fed agriculture is also significantly impacted as pastures will experience depleted water availability from soil moisture through both the warm season and winter cropping.

5.2.2 Storyline 2– Increases in cool-season runoff, decreases in warm-season soil moisture (MIROC5_QME RCP8.5)

This storyline represents some increase in cool-season runoff (12%), and a moderate decrease in warm-season soil moisture (−7%). This storyline is one of the more favourable in terms of increased water availability.

The cool-season runoff increases in the storage catchment are driven by projected increases in precipitation (3%). Soil moisture is projected to decrease in the catchment in the cool months. This suggests that the increases in runoff may be associated with precipitation occurring in the form of higher-intensity events, which would generate more runoff.

Warm-season precipitation is also projected to increase by around 10 mm a season. However, little change is projected in warm-season runoff in the storage catchments, so the increased precipitation is not likely to increase storage infilling. The result of higher-intensity precipitation and runoff occurring over a drier catchment (indicated by reduced soil moisture) could be less water available for filling groundwater and supporting baseflows. Under this scenario, infilling may become more associated with extreme precipitation events, but there could be less baseflow to sustain storage infilling in average conditions. This change in hydrology will also reduce infilling during natural periods of below-average precipitation.

Combined with projected increases in demand, this more favourable storyline could see water availability becoming less secure due to the shift in hydrology described above. This could result in more water being supplied via supplementary or unallocated flow events from flood harvesting rather than more secure allocations from water storages.

5.3 Conclusions

National Hydrological Projections for changes to precipitation, soil moisture, runoff and evapotranspiration can be useful indicators for a range of water-sensitive impacts, such as water availability for the environment and human consumption, inflows and demands on water storages, and soil moisture for rain-fed agriculture or as a risk factor for bushfires. Using a storylines approach, we have used the National Hydrological Projections to interrogate potential changes to water security as an example of how impact risks can be assessed with these data. Each of

the 16 ensemble members represents a plausible future storyline with respect to future changes to water security. Results from other projections are discussed to contextualise where these storylines fit in a broader understanding of plausible futures.

6 Acknowledgements

We acknowledge the work and support of the CSIRO CCAM model development team, including CSIRO Oceans and Atmospheres and CSIRO High Performance Computing along with partners, for their work producing, coordinating and making available the CCAM 50 km datasets required for this project. We thank Marcus Thatcher from the CCAM development team for their useful discussions around accessing, using, and interpreting these data.

We acknowledge the work and support of Dr Fiona Johnson, Dr Raj Mehrotra and Professor Ashish Sharma from the University of New South Wales School of Civil and Environmental Engineering for their roles in producing the MRNBC bias-correction methodology and for their useful discussion around implementing and interpreting this method.

For their roles in producing, coordinating, and making available the ISIMIP2b input data and impact model output, we acknowledge the modelling groups, the ISIMIP2b sector coordinators and the ISIMIP2b cross-sectoral science for the useful discussions around implementing the ISIMIP2b bias-correction methodology. We acknowledge the work and support of Dr Andrew Dowdy from the Australian Bureau of Meteorology producing and making available the QME bias-correction methodology and bias-corrected model input data.

We acknowledge the World Climate Research Programme's Working Group on Coupled Modelling, which is responsible for CMIP, and we thank the climate modelling groups (listed in Table 3.1 of this report) for producing and making available their model output. For CMIP, the US Department of Energy's Program for Climate Model Diagnosis and Intercomparison provides coordinating support and led development of software infrastructure in partnership with the Global Organization for Earth System Science Portals. This research project was undertaken with the assistance of resources and services from the National Computational Infrastructure (NCI), which is supported by the Australian Government. We thank Dr Kelsey Druken and Dr Yiling Liu for their support in providing the National Hydrological Projections foundational dataset as part of the NCI Data Collection.

The National Hydrological Project has been realised through the hard work and effort of the project team and the support of many individuals from the Australian Bureau of Meteorology, who we would like to thank: for project sponsorship and general project guidance, Dr Robert Argent, Jeff Perkins, Matt Coulton and Dr Elisabetta Carrara; for project management, Zeina Assouad and Anastasia Li; for her leadership while transitioning the product into a service, Elizabeth McDonald; for scientific leadership, Dr Pandora Hope and Dr Justin Peter on climate trends and modelling, and Dr Sugata Narsey on the storylines approach; for support in data processing and software development Dr Justin Peter, Dr Wendy Sharples, Vi Co Duong, Dr Greg Kociuba, Jake Roussis and others; James Devonshire for plotting maps, the Australian Water Outlook team that built the user interface to access National Hydrological Projections data, Khadiza Tahera, Subash Sharma, Ross Lillis, Kieran Lomas and Mark Menzel; for general guidance on the AWRA-L hydrological impact model, Dr Andrew Frost, Dr Ashkan Shokri and Stuart Barron-Hay; and for their general support, Katy Bahramian, Dr Ali Azarnivand and Dr Chris Ruediger. A special thanks to Dr Chantal Donnelly and Dr Louise Wilson who initiated and initially led the project.

We thank deeply all the lead and contributing authors named in the hydrological assessment reports for their large and continuous efforts in producing the hydrological assessment reports. We would like to acknowledge the tireless efforts of Dr Ulrike Bende-Michl who led the National Hydrological Project, developed, directed the scientific content of the hydrological assessment reports, and coordinated the report writing and reviews as well as being a lead contributing author. We would like to thank Dr Alison Oke greatly for her huge efforts in managing the hydrological assessment report writing, developing the report structure and scientific content as well as being lead contributing author. Thanks also to Dr Justin Peter and Dr Greg Kociuba who have developed and operationalised the graphs and plots underpinning the reports. We acknowledge Dr Sri Srikanthan for strengthening and fortifying the reports and Dr Vjekoslav Matic for developing the storylines.

This report benefited from the comments provided by several reviewers, including Drs Chiara Holgate, Ian Watterson, Mark Kennard, Masoud Edraki, Mitchell Black, Mohammed Bari, Murray Peel, Sugata Narsey, Andrew

Dowdy, Sunny Yu, Surendra Rauniyar as well as Artemis Kitsios, Graham Green, Jacqueline Schopf, Jacquie Bellhouse, Jacqui Russel, Susannah Clement and Timothy William Bond.

We also acknowledge the useful discussions with Dr Ramona Dalla Pozza and Geoff Steendam and teams from the Victorian State Government Department of Environment, Land, Water and Planning; and the useful discussions with Matthew Reilly from the New South Wales Department of Planning, Industry and Environment.

We acknowledge and are grateful for the participation of the Western Australian Department of Water and Environmental Regulation and Water Corporation WA in demonstration cases, including Artemis Kitsios, Jacquie Bellhouse and Jacqueline Schopf, and the useful discussions with Dr Francis Chew, Dr Steve Charles and Dr Nick Potter from CSIRO Land and Water.

We thank Dr Margot Turner for developing the National Hydrological Projections demonstration use cases in collaboration with state departments that also helped to inform the hydrological assessment reports.

We acknowledge PaperGiant for their consulting effort in the user centred design of the Australian Water Outlook portal and all the contributing participants from multiple organisations.

We thank Margie Beilharz from The Open Desk greatly for her editorial support.

7 References

Abbs, DJ & Rafter, AS 2009, *Impact of climate variability and climate change on rainfall extremes in Western Sydney and surrounding areas: Component 4 – dynamical downscaling*, Report to the Sydney Metro Catchment Management Authority and Partners, CSIRO, Aspendale.

Adapt NSW n.d. *Climate projections for NSW*, Adapt NSW website, accessed 28 October 2021 <https://climatechange.environment.nsw.gov.au/Climate-projections-for-NSW/>.

Alam, MA, Emura, K, Farnham, C & Yuan, J 2018, 'Best-fit probability distributions and return periods for maximum monthly rainfall in Bangladesh', *Climate*, vol. 6, no. 1.

Alexander, LV & Arblaster, JM 2009, 'Assessing trends in observed and modelled climate extremes over Australia in relation to future projections', *International Journal of Climatology*, vol. 29, no. 3, pp. 417–435.

Ashok, K, Guan, Z & Yamagata, T 2003, 'Influence of the Indian Ocean Dipole on the Australian winter rainfall', *Geophysical Research Letters*, vol. 30, no. 15.

Azarnivand, A, Sharples, W, Bende-Michl, U, Shokri, A, Srikanthan, S, Frost, AJ & Baron-Hay, S 2021, *Uncertainty analysis of modelling hydrologic states using AWRA-L – understanding impacts from parameter uncertainty for the National Hydrological Projections*. *Hydrological Projections Project*. Bureau of Meteorology, Bureau Research Report 060, Melbourne. <http://www.bom.gov.au/research/publications/researchreports/BRR-060.pdf>.

Bali, TG 2003, 'The generalized extreme value distribution', *Economics Letters*, vol. 79, no. 3, pp. 423–427.

Brown, JR, Moise, AF, Colman, R & Zhang, H 2016, 'Will a warmer world mean a wetter or drier Australian monsoon?', *Journal of Climate*, vol. 29, no. 12, pp. 4577–4596.

Bureau of Meteorology 2020, *National Water Account*, Bureau of Meteorology website, accessed 11 November 2021, <http://www.bom.gov.au/water/nwa/2020/>.

Cai, W, Cowan, T & Sullivan, A 2009, 'Recent unprecedented skewness towards positive Indian Ocean Dipole occurrences and its impact on Australian rainfall', *Geophysical Research Letters*, vol. 36, no. 11.

CCiA (Climate Change in Australia) n.d. a, *Climate change in Australia: climate information, projections, tools and data*, CCiA website, accessed 28 October 2021, <www.climatechangeinaustralia.gov.au>.

CCiA (Climate Change in Australia) n.d. b, *Clusters*, CCiA website, accessed 4 November 2021, <https://www.climatechangeinaustralia.gov.au/en/projections-tools/regional-climate-change-explorer/clusters/>.

CCiA (Climate Change in Australia) 2020, *Victorian Climate Projections 2019*, CCiA website, accessed 18 September 2021, <https://www.climatechangeinaustralia.gov.au/en/projects/victorian-climate-projections-2019/>.

Chiew, FHS 2006, 'Estimation of rainfall elasticity of streamflow in Australia', *Hydrological Sciences Journal*, vol. 51, no. 4, pp. 613–625.

Collier, M & Uhe, P 2012, *CMIP5 datasets from the ACCESS1.0 and ACCESS1.3 coupled climate models*, Centre for Australian Weather and Climate Research (CAWCR) Technical Report no. 059. CSIRO and Bureau of Meteorology, Australia.

CSIRO & Bureau of Meteorology 2015, *Climate change in Australia projections for Australia's natural resource management regions: technical report*. CSIRO and Bureau of Meteorology, Australia.

CSIRO & Bureau of Meteorology 2020, *State of the climate 2020*, Commonwealth of Australia.

DELWP (Department of Environment, Land, Water and Planning), Bureau of Meteorology, CSIRO and The University of Melbourne 2020, *Victoria's water in a changing climate*, State of Victoria, DELWP.

DELWP (Department of Environment, Land, Water and Planning) 2016, *Guidelines for assessing the impact of climate change on water supplies in Victoria*, State of Victoria, DELWP.

DELWP (Department of Environment, Land, Water and Planning) n.d. *Victorian Water and Climate Initiative (2017–2020)*, DELWP website, accessed 28 October 2021, <https://www.water.vic.gov.au/climate-change/climate-and-water-resources-research/the-victorian-water-and-climate-initiative>.

DELWP (Department of Environment, Land, Water and Planning) 2020, *Guidelines for assessing the impact of climate change on water supplies in Victoria*, State of Victoria, DELWP.

Dowdy, AJ & Catto JL 2017. 'Extreme weather caused by concurrent cyclone, front and thunderstorm occurrences', *Scientific Reports*, vol. 7, 40359, doi:10.1038/srep40359

Dowdy, AJ 2020, 'Seamless climate change projections and seasonal predictions for bushfires in Australia', *Journal of Southern Hemisphere Earth Systems Science*, vol. 70, no. 1, pp. 120–138.

Drosdowsky, W 2005, 'The latitude of the subtropical ridge over eastern Australia: the L index revisited', *International Journal of Climatolology*, vol. 25, pp. 1291–1299, doi:10.1002/joc.1196

Dunne, JP, John, JG, Adcroft, AJ et al. 2012, 'GFDL's ESM2 global coupled climate-carbon earth system models. Part I: Physical formulation and baseline simulation characteristics', *Journal of Climate*, vol. 25, no. 19, pp. 6646–6665.

Easterling, DR, Meehl, GA, Parmesan, C, Changnon, SA, Karl, TR & Mearns, LO 2000, 'Climate extremes: observations, modeling, and impacts', *Science*, vol. 289, no. 5487, pp. 2068–2074.

Fowler, HJ & Ekström, M 2009, 'Multi-model ensemble estimates of climate change impacts on UK seasonal precipitation extremes', *International Journal of Climatology*, vol. 29, no. 3, pp. 385–416.

Frost, AJ & Wright, DP 2018, *Evaluation of the Australian Landscape Water Balance model: AWRA-L v6*. Bureau of Meteorology Technical Report, Commonwealth of Australia.

Frost, AJ, Ramchurn A & Smith A 2018, *The Australian Landscape Water Balance model (AWRA-L v6)*: *technical description of the Australian Water Resources Assessment Landscape model version 6.* Bureau of Meteorology Technical Report.

Fu, G, Charles, SP & Chiew, FHS 2007, 'A two-parameter climate elasticity of streamflow index to assess climate change effects on annual streamflow', *Water Resources Research*, vol. 43, no. 11, p. W11419.

Gallant, AJE, Hennessy, KJ & Risby, J 2007, 'Trends in rainfall indices for six Australian regions: 1910–2005', *Australian Meteorological Magazine*, vol. 56, pp. 223–239.

Goyder Institute for Water Research (n.d.) *Research focus: climate change*, Goyder Institute website, accessed 28 October 2021, <http://www.goyderinstitute.org/research/foundation-research/climate-change/>.

Greve, P, Roderick, ML & Seneviratne, SI 2017, 'Simulated changes in aridity from the last glacial maximum to 4xCO_2', *Environmental Research Letters*, vol. 12, no. 11, p. 114021.

Grose, MR, Moise, AF, Timbal, B, Katzfey, JJ, Ekström, M & Whetton, PH 2015, 'Climate projections for southern Australian cool-season rainfall: insights from a downscaling comparison', *Climate Research*, vol. 62, no. 3, pp. 251–265.

Grose, MR, Risbey JS, Moise AF, Osbrough S, Heady C, Wilson L and Erwin, T 2017, 'Constraints on southern Australian precipitation change based on atmospheric circulation in CMIP5 simulations', *Journal of Climate*, vol. 30, no. 1, pp. 225–242, doi:10.1175/JCLI-D-16-0142.1

Grose, MR, Syktus, J, Thatcher, M, Evans, JP, Ji, F, Rafter, T and Remenyi, T 2019, 'The role of topography on projected rainfall change in mid-latitude mountain regions', *Climate Dynamics*, vol. 53, no. 5–6, pp. 3675–3690.

Hempel, S, Frieler, K, Warszawski, L, Schewe, J & Piontek, F 2013, 'A trend-preserving bias correction – the ISI-MIP approach', *Earth System Dynamics*, vol. 4, no. 2, pp. 219–236.

Hope, P and Watterson, I 2018, 'Persistence of cool conditions after heavy rain in Australia', *Journal of Southern Hemisphere Earth Systems Science*, vol. 68, no. 1, pp. 41 – 64.

Hope, P, Grose, MR, Timbal, B et al. 2015, 'Seasonal and regional signature of the projected southern Australian rainfall reduction', *Australian Meteorological and Oceanographic Journal*, vol. 65, no. 1, pp. 54–71.

Hope, P, Timbal, B, Hendon, H, Ekström, M and Potter, N 2017, *A synthesis of findings from the Victorian Climate Change Iniative (VicCI)*, Bureau of Meteorology, Australia, <http://www.bom.gov.au/research/projects/vicci/>

Johnson, AKL & Murray, AE 2004, 'Modelling the spatial and temporal distribution of rainfall: a case study in the wet and dry tropics of North East Australia', *Australian Geographer*, vol. 35, no. 1, pp. 39–57.

Johnson, F & Sharma, A 2012, 'A nesting model for bias correction of variability at multiple time scales in general circulation model precipitation simulations', *Water Resources Research*, vol. 48, no. 1.

Jones, DA, Wang, W & Fawcett, R 2009, 'High-quality spatial climate data-sets for Australia', *Australian Meteorological and Oceanographic Journal*, vol. 58, no. 4, pp. 233–248.

McBride, JL & Nicholls, N 1983, 'Seasonal relationships between Australian rainfall and the Southern Oscillation', *Monthly Weather Review*, vol. 111, no. 10, pp. 1998–2004.

McKee, TB, Doesken, NJ, Kleist, J 1993, 'The relationship of drought frequency and duration of time scales', *Proceedings of the Eighth Conference on Applied Climatology*, American Meteorological Society, Boston, pp. 179–184.

Mehrotra, R & Sharma, A 2016, 'A multivariate quantile-matching bias correction approach with auto- and cross-dependence across multiple time scales: implications for downscaling', *Journal of Climate*, vol. 29, no. 10, pp. 3519–3539.

Milly, PCD, Wetherald, RT, Dunne, KA & Delworth, TL 2002, 'Increasing risk of great floods in a changing climate', *Nature*, vol. 415, no. 6871, pp. 514–517.

Moise, A, Wilson, L, Grose, M et al. 2015, 'Evaluation of CMIP3 and CMIP5 models over the Australian region to inform confidence in projections', *Australian Meteorological and Oceanographic Journal*, vol. 65, no. 1, pp. 19–53.

Nash, JE & Sutcliffe, JV 1970, 'River flow forecasting through conceptual models part I – A discussion of principles', *Journal of Hydrology*, vol. 10, no. 3, pp. 282–290.

Palmer, TN & Räisänen, J 2002, 'Quantifying the risk of extreme seasonal precipitation events in a changing climate', *Nature*, vol. 415, no. 6871, pp. 512–514.

PCMDI (Program for Climate Model Diagnosis & Intercomparison) 2021, *CMIP5 – Coupled Model Intercomparison Project Phase 5 – Overview*, PCMDI website, accessed 10 November 2021, <https://pcmdi.llnl.gov/mips/cmip5/>.

Pepler, A, Ashcroft, L & Trewin, B 2018, The relationship between the subtropical ridge and Australian temperatures. *Journal of Southern Hemisphere Earth System Science*, vol. 68, pp. 201–214, doi:10.22499/3.6801.011

Pepler, AS, Dowdy, AJ, van Rensch, P, Rudeva, I, Catto, JL & Hope, P 2020, 'The contributions of fronts, lows and thunderstorms to southern Australian rainfall', *Climate Dynamics*, vol. 55, no. 5–6, pp. 1489–1505.

Rafter, AS & Abbs, DJ 2009, 'An analysis of future changes in extreme rainfall over Australian regions based on GCM simulations and Extreme Value Analysis', *CAWCR Research Letters*, vol. 3, pp. 43–48.

Rafter, T, Trenham, C, Thatcher, M, Remenyi, T, Wilson, L, Heady, C & Love, P 2019, *CCAM Climate Downscaling Data for Victoria 2019*, CSIRO Data Access Portal website, accessed 10 November 2021, <https://data.csiro.au/collection/38583>.

Reid, KJ, Simmonds, I, Vincent, CL, & King, AD 2019, 'The Australian northwest cloudband: climatology, mechanisms, and association with precipitation', *Journal of Climate,* vol. 32, no. 20, pp. 6665–6684.

Risbey, JS, Pook, MJ, McIntosh, PC, Ummenhofer, CC & Meyers, G 2009, 'Characteristics and variability of synoptic features associated with cool season precipitation in southeastern Australia', *International Journal of Climatology*, vol. 29, pp. 1595–1613.

SEACI (South Eastern Australian Climate Initiative) n.d. *The South Eastern Australian Climate Initiative*, SEACI website, accessed 28 October 2021, <http://www.seaci.org/>.

Sherwood, SC, Roca, R, Weckwerth, TM & Andronova, NG 2010, 'Tropospheric water vapor, convection, and climate', *Reviews of Geophysics*, vol. 48, no. 2.

Srikanthan, S., Bende-Michl, U, Sharples, W et al. 2022, *Introduction to the National Hydrological Projections Project*, Bureau of Meteorology, Bureau Research Report 061, Melbourne.

Suppiah, R 1992, 'The Australian summer monsoon: a review', *Progress in Physical Geography: Earth and Environment*, vol. 16, no. 3, pp. 283–318.

Taylor, KE, Stouffer, RJ & Meehl, GA 2012, 'An overview of CMIP5 and the experiment design', *Bulletin of the American Meteorological Society*, vol. 93, no. 4, pp. 485–498.

Timbal, B, Abbs, D, Bhend, J et al. 2015, *Murray Basin cluster report*, Climate Change in Australia Projections for Australia's Natural Resource Management Regions: Cluster Reports, M Ekström, P Whetton, C Gerbing et al. (eds), CSIRO and Bureau of Meteorology, Australia.

Ukkola, AM, Pitman, AJ, De Kauwe, MG, Abramowitz, G, Herger, N, Evans, JP & Decker, M 2018, 'Evaluating CMIP5 model agreement for multiple drought metrics', *Journal of Hydrometeorology*, vol. 19, no. 6, pp. 969–988.

Voldoire, A, Sanchez-Gomez, E, Salas y Mélia, D et al. 2013, 'The CNRM-CM5.1 global climate model: description and basic evaluation', *Climate Dynamics*, vol. 40, no. 9–10, pp. 2091–2121.

Walsh, KJE & Ryan, BF 2000, 'Tropical cyclone intensity increase near Australia as a result of climate change', *Journal of Climate*, vol. 13, no. 16, pp. 3029–3036.

Wang, G, Cai, W & Santoso, A 2017, 'Assessing the impact of model biases on the projected increase in frequency of extreme positive Indian Ocean Dipole events', *Journal of Climate*, vol. 30, no. 8, pp. 2757–2767.

Wang, GQ, Zhang, JY, Xu, YP, Bao, ZX and Yang, XY 2017, 'Estimation of future water resources of Xiangjiang River Basin with VIC model under multiple climate scenarios', *Water Science and Engineering,* vol. 10, no. 2, pp. 87–96.

Wasko, C & Nathan, R 2019, 'Influence of changes in rainfall and soil moisture on trends in flooding', *Journal of Hydrology*, vol. 575, pp. 432–441.

Wasko, C & Sharma, A 2017, 'Global assessment of flood and storm extremes with increased temperatures', *Scientific Reports*, vol. 7, no. 1, 7945.

Wasko, C, Shao, Y, Vogel, E, Wilson, L, Wang, QJ, Frost, A & Donnelly, C 2021, 'Understanding trends in hydrologic extremes across Australia', *Journal of Hydrology*, vol. 593, p. 125877.

Watanabe, M, Suzuki, T, O'ishi, R, et al. 2010, 'Improved climate simulation by MIROC5: mean states, variability, and climate sensitivity', *Journal of Climate*, vol. 23, no. 23, pp. 6312–6335.

Wheeler, MC, Hendon, HH, Cleland, S, Meinke, H & Donald, A 2009, 'Impacts of the Madden–Julian Oscillation on Australian rainfall and circulation', *Journal of Climate*, vol. 22, no. 6, pp. 1482–1498.

Yang, Y, Roderick, ML, Zhang, S, McVicar, TR & Donohue, RJ 2019 'Hydrologic implications of vegetation response to elevated CO_2 in climate projections', *Nature Climate Change*, vol. 9, no. 1, pp. 44–48.

Yin, J, Guo, S, Gu, L, He, S, Ba, H, Tian, J, Li, Q & Chen, J 2020, 'Projected changes of bivariate flood quantiles and estimation uncertainty based on multi-model ensembles over China', *Journal of Hydrology*, vol. 585, p. 124760.

Zhang, XS, Amirthanathan, GE, Bari, MA et al. 2016, 'How streamflow has changed across Australia since the 1950s: evidence from the network of hydrologic reference stations', *Hydrology and Earth System Sciences*, vol. 20, no. 9, pp. 3947–3965.

8 Appendix: Evaluation of bias-correction methods

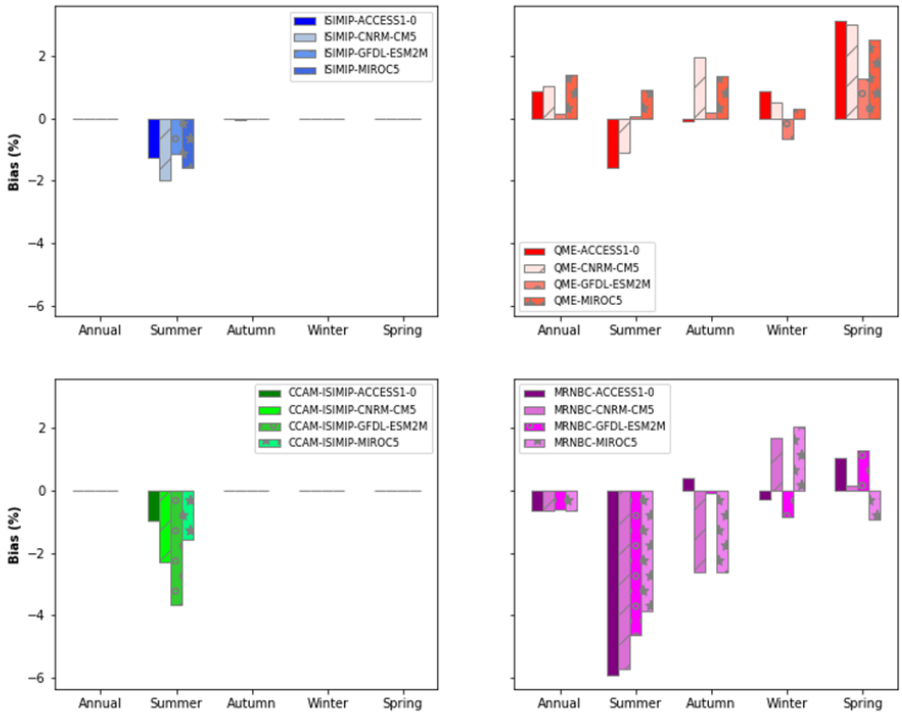

Figure 8.1. Bias (%) in mean annual and seasonal precipitation for the Murray Basin region

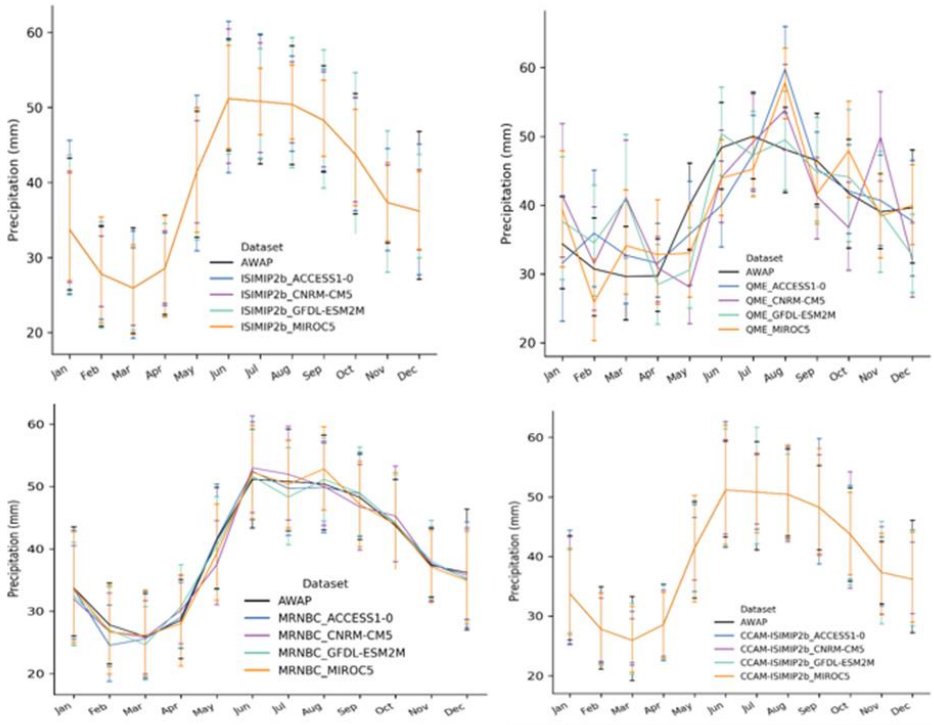

Figure 8.2. Comparison of the mean monthly precipitation (mm) for the 16 ensemble members and observed (AWAP) data for the Murray Basin region (1976–2005)

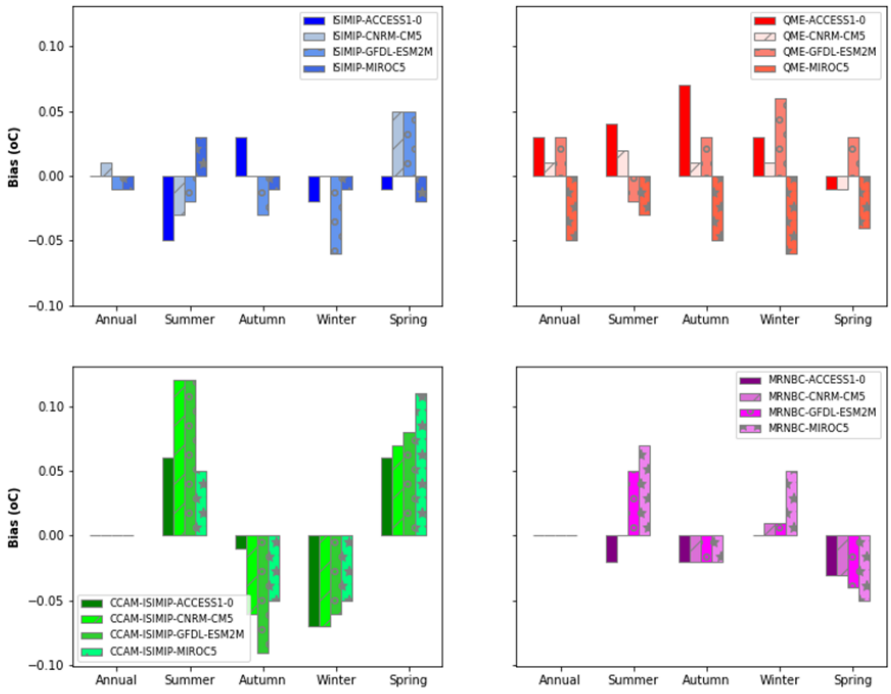

Figure 8.3. Bias (°C) in mean annual and seasonal maximum temperature for the Murray Basin region

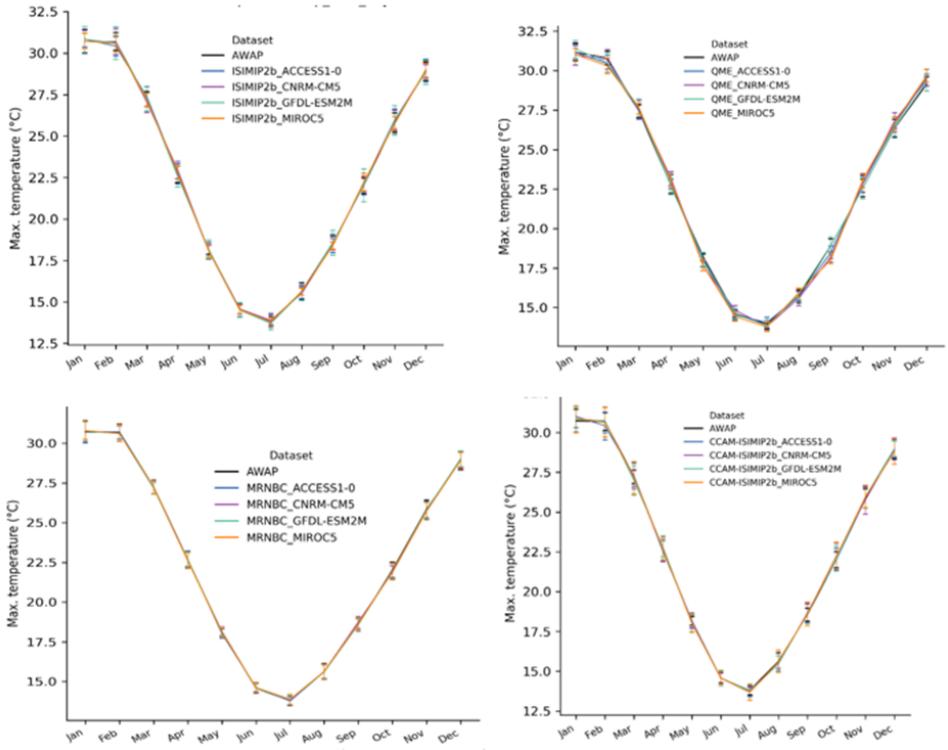

Figure 8.4. Comparison of the mean monthly maximum temperature (°C) for the 16 ensemble members and observed (AWAP) data for the Murray Basin region (1976–2005)

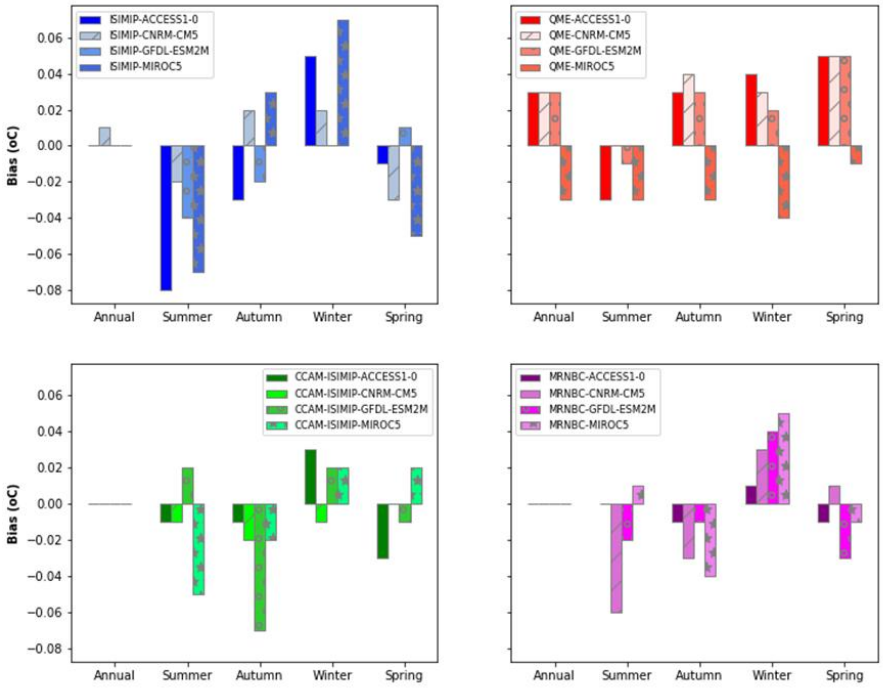

Figure 8.5. Bias (°C) in mean annual and seasonal minimum temperature for the Murray Basin region

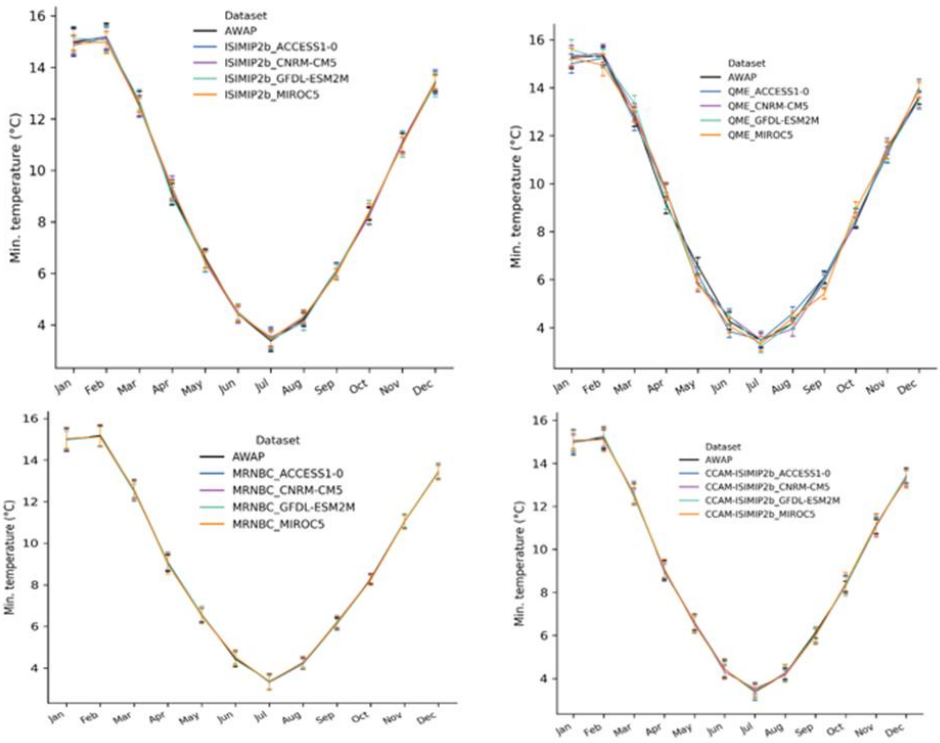

Figure 8.6. Comparison of the mean monthly minimum temperature (°C) for the 16 ensemble members and observed (AWAP) data for the Murray Basin region (1976–2005)

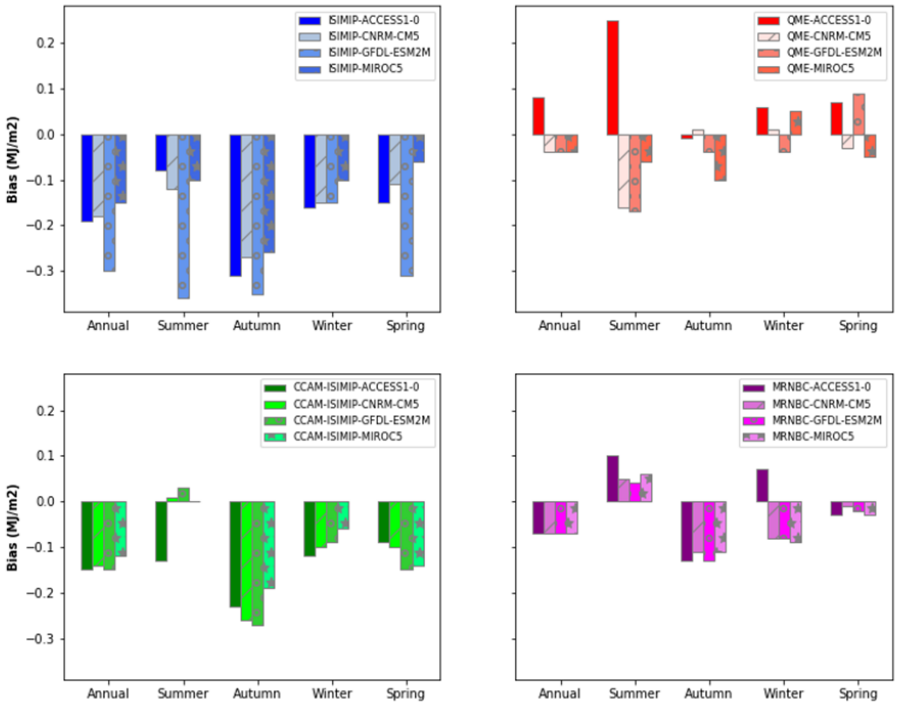

Figure 8.7. Bias (MJ/m2) in mean annual and seasonal solar radiation for the Murray Basin region

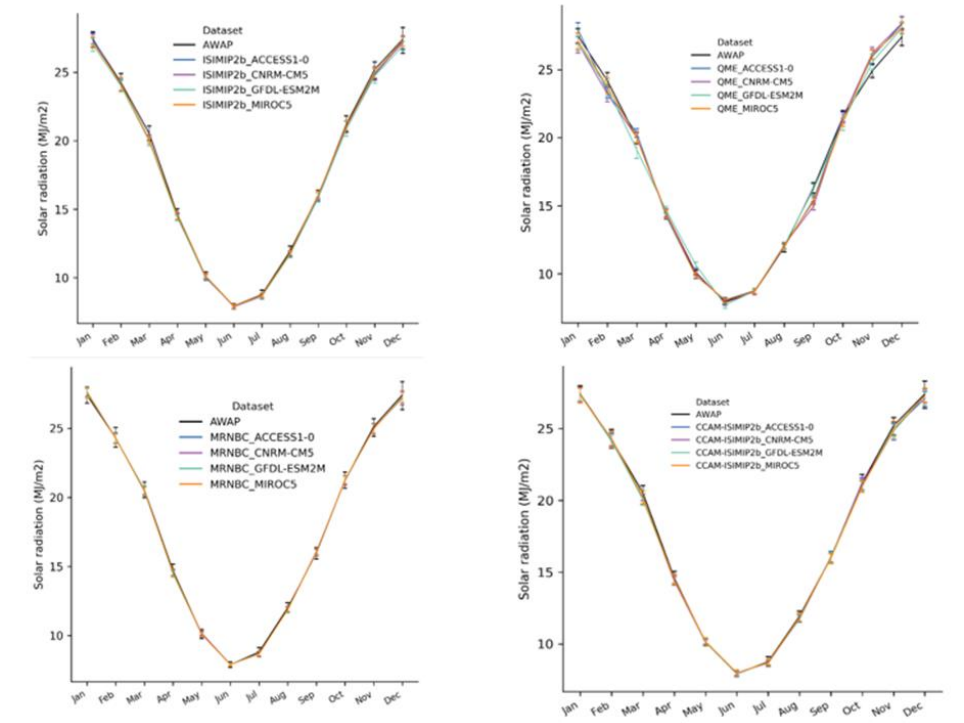

Figure 8.8. Comparison of the mean monthly solar radiation (MJ/m2) for the 16 ensemble members and observed (AWAP) data for the Murry Basin region (1976–2005)

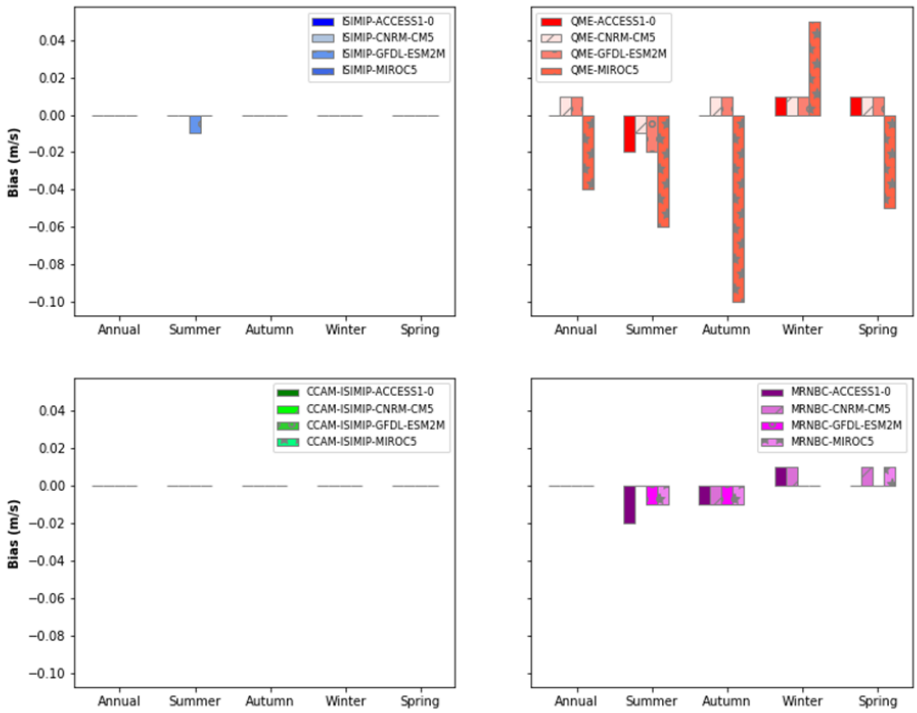

Figure 8.9. Bias (m/s) in mean annual and seasonal wind speed for the Murray Basin region

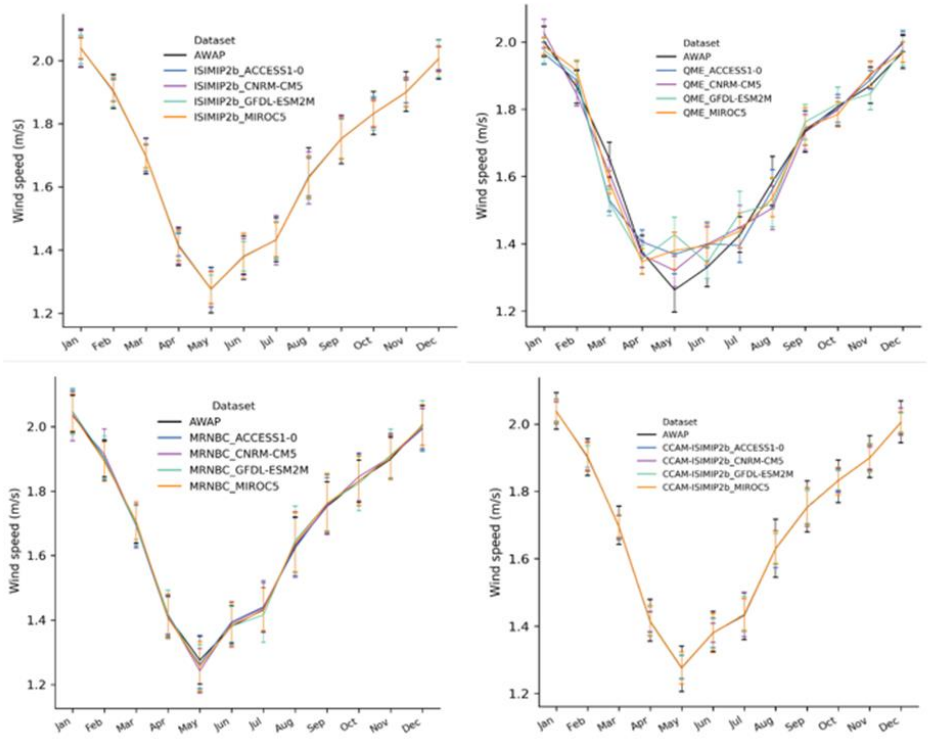

Figure 8.10. Comparison of the mean monthly wind speed (m/s) for the 16 ensemble members and observed (AWAP) data for the Murray Basin region (1976–2005)

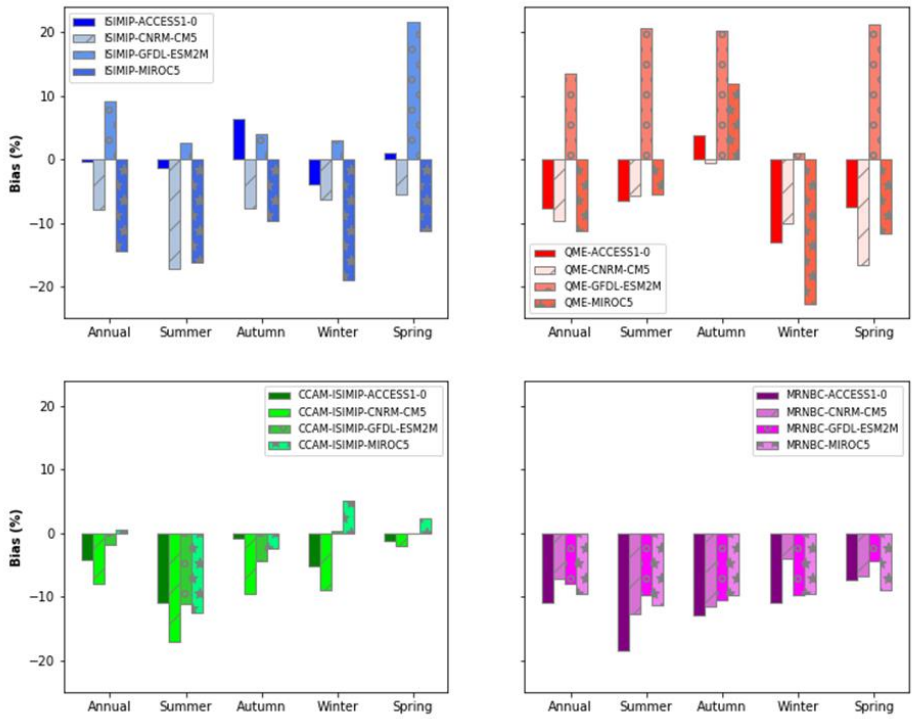

Figure 8.11. Bias (%) in mean annual and seasonal runoff for the Murray Basin region

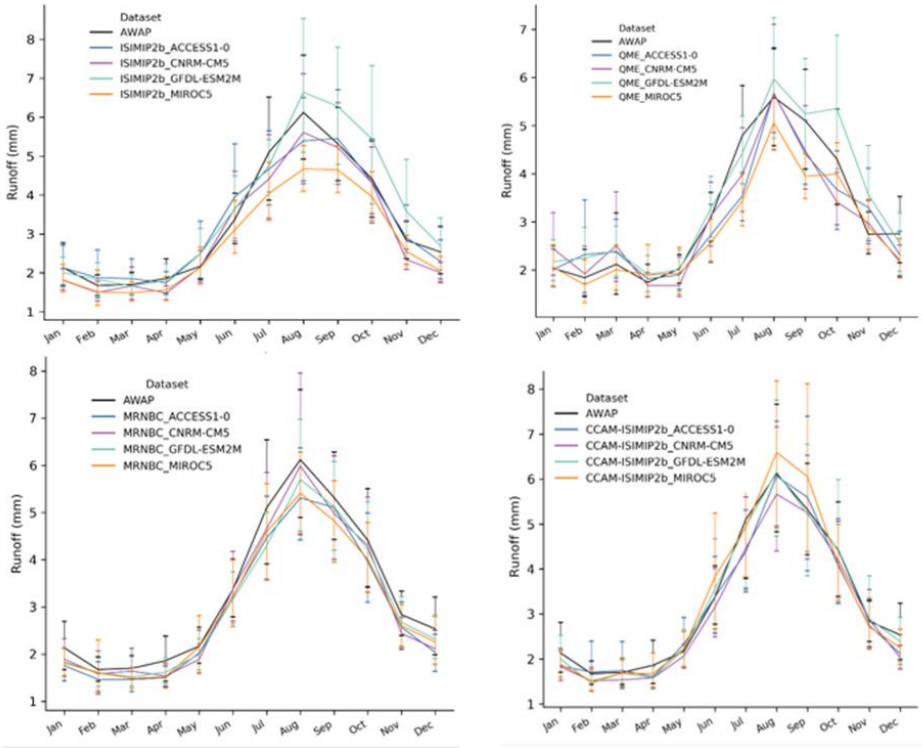

Figure 8.12. Comparison of the mean monthly runoff (mm) for the 16 ensemble members and observed (AWAP) data for the Murray Basin region (1976–2005)

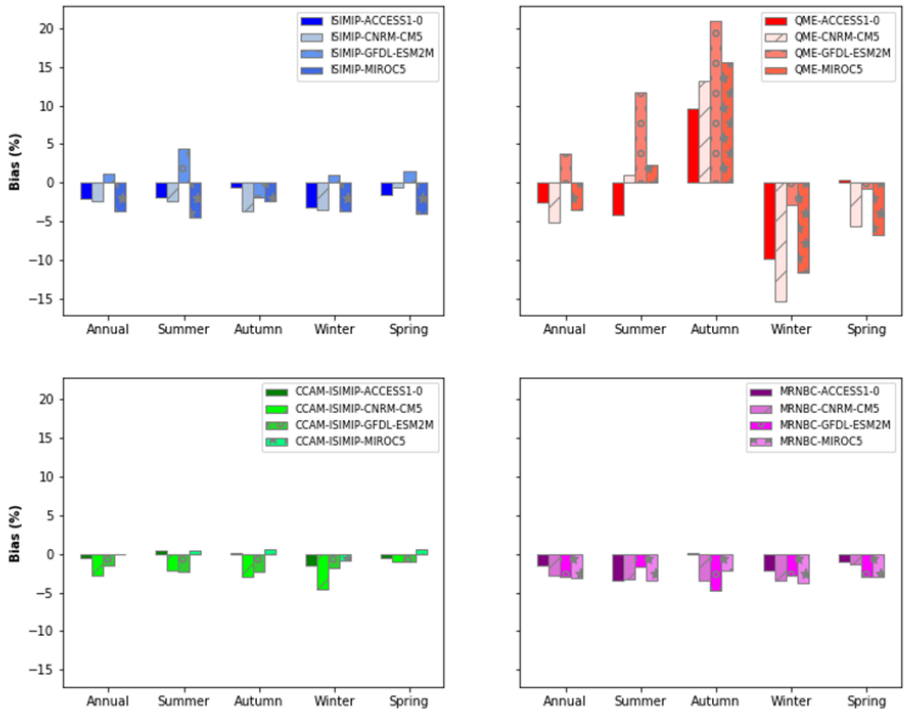

Figure 8.13. Bias (%) in mean annual and seasonal soil moisture for the Murray Basin region

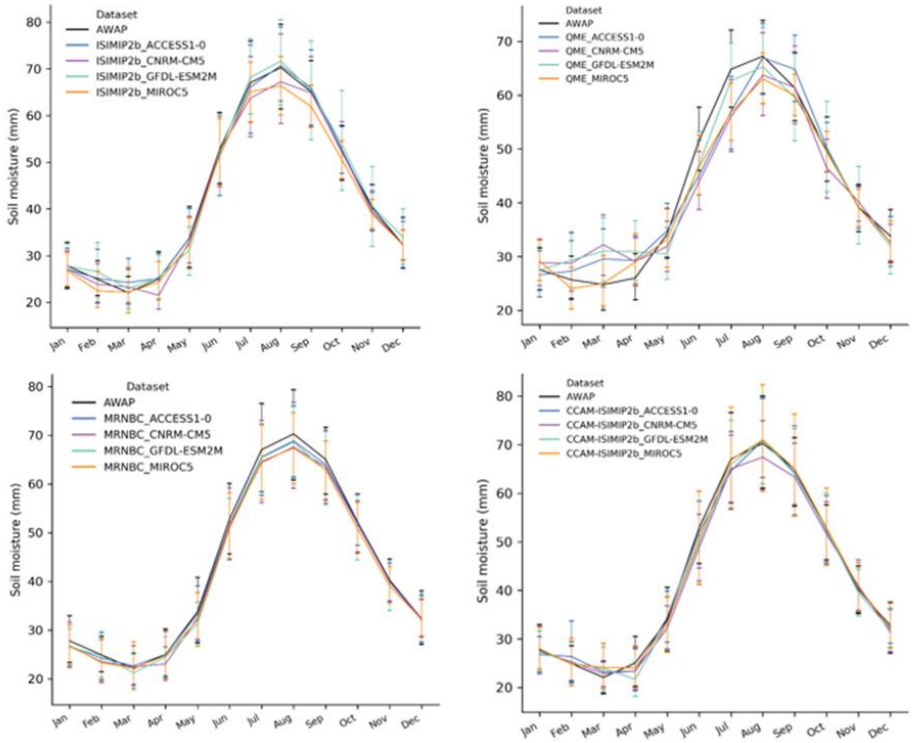

Figure 8.14. Comparison of the mean monthly soil moisture (mm) for the 16 ensemble members and observed (AWAP) data for the Murray Basin region (1976–2005)

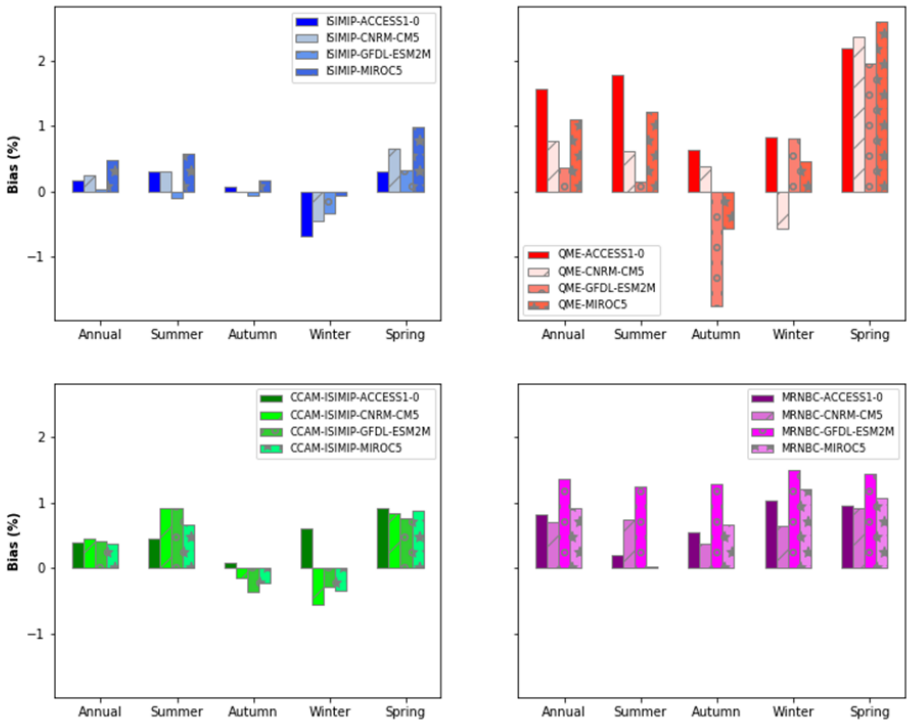

Figure 8.15. Bias (%) in mean annual and seasonal potential evapotranspiration for the Murray Basin region

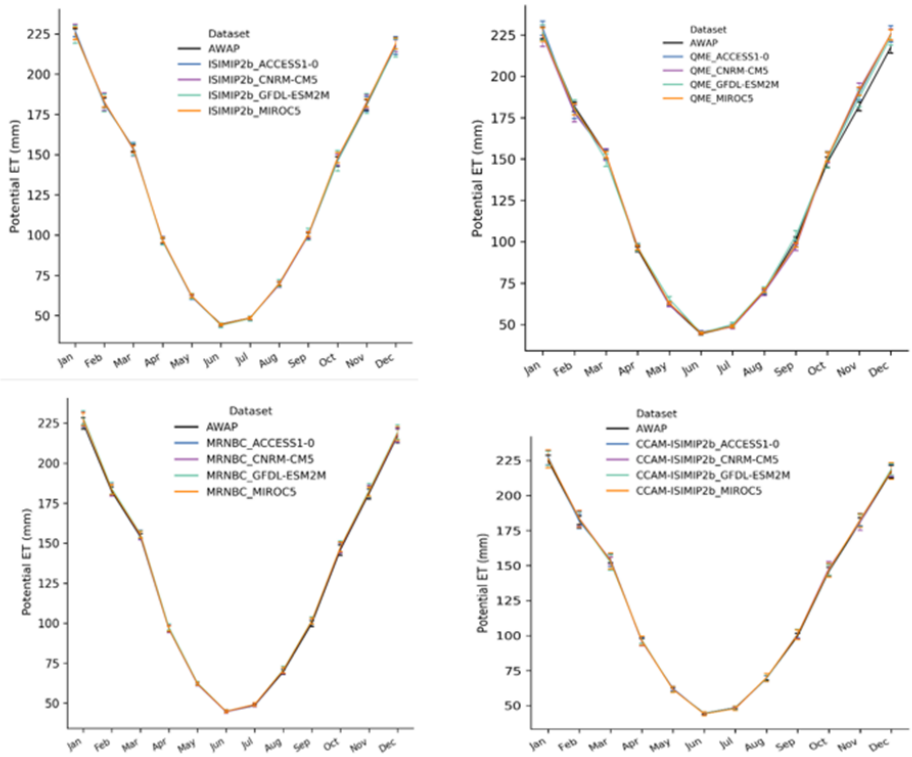

Figure 8.16. Comparison of the mean monthly potential evapotranspiration (mm) for the 16 ensemble members and observed (AWAP) data for the Murray Basin region (1976–2005)